4.2.5.10. 10h (Man2HMC24). ^{1}H-NMR (400 MHz, CD$_3$OD): δ 0.89 (6H, t, J = 6.9 Hz, methyl), 1.30 (62H, brs, methylene), 1.55–1.62 (2H, m, methylene), 1.65–1.75 (2H, m, methylene), 2.19 (2H, t, J = 7.4 Hz, methylene), 3.47–4.00 (10H, m), for mannose C2, C3, C4, C5, C6a, C6b, sphingosine C1a, C1b, C2 and C3, 4.72–4.74 (1H, m, anomeric), 7.2 (1H, m, amide).

High resolution ESI-MS calculated for C$_{47}$H$_{93}$N$_1$O$_8$Na (M + Na)$^+$, 822.6799; found 822.6813.

4.2.5.11. 10i (Man2HMC16). ^{1}H-NMR (400 MHz, CD$_3$OD): δ 0.82–0.94 (6H, m, methyl), 1.28 (48H, brs, methylene), 1.53–1.63 (2H, m, methylene), 1.63–1.78 (2H, m, methylene), 2.15–2.21 (2H, m, methylene), 3.40–3.95 (10H, m), for mannose C2, C3, C4, C5, C6a, C6b, sphingosine C1a, C1b, C2 and C3, 4.78–4.85 (1H, m, anomeric), 7.2 (1H, m, amide).

High resolution FAB-MS, calculated for C$_{39}$H$_{78}$ N$_1$O$_8$ (M + H)$^+$, 688.5727; found 688.5733.

4.2.6   3-Hydroxy   α-ManCer   3-Hydroxy   α-ManCer (Man3OHCl6, Scheme 3) was prepared as previously reported [8].

4.3. Bioassay of the synthesized glycolipids

Vα19-Jα26 invariant TCR Tg mice with the TCR Cα-deficient background were established as described previously [7, 8]. C57BL/6 mice were obtained from Sankyo Service Co. (Tokyo, Japan) and Jackson Laboratory (Bar Harbor, ME, USA). MNCs were prepared from single cell suspensions of mouse livers by density gradient centrifugation using Percoll (Pharmacia, Uppsala, Sweden) as described previously [3]. Liver MNCs from indicated mouse strains (2–4 months of age) were cultured in 200 μl of DMEM supplemented with 10% FCS, 100 U ml^{-1} penicillin, 50 μg ml^{-1} streptomycin and 5 × 10^{-5} M 2-ME in the presence of glycolipids dissolved in DMSO (final concentration, 2 μg ml^{-1}). The concentration of cytokines in the culture fluid was determined by ELISA after 2 days (Pharmingen, San Diego, CA, USA). Cell proliferation was assessed at day 2 of culture by measuring the incorporation of [^{3}H]-thymidine (0.5 μCi ml^{-1}, Amersham, Buckinghamshire, UK) for 5 h.

Stimulation of lymphocytes in vivo was performed as previously reported by Yoshimoto et al. [25]. Vα19 Tg$^+$ TCR α$^{-/-}$ or C57BL/6 mice (8 ~ 20 w of age) were intravenously injected with glycolipids (20 μg per 200 μl PBS) instead of anti-CD3 antibody. Spleens were removed from mice 90 min after the injection. MNCs were immediately prepared from them by density gradient centrifugation using lymphosepar II (MBL, Gunma, Japan, d = 1.090). They were cultured in the DMEM (10^7 cells per ml). Cytokines in the culture fluid were determined by ELISA.

References

[1] H.R. MacDonald, J. Exp. Med. 182 (1995) 630–638.

[2] A. Bendelac, M.N. Rivera, S.H. Park, J.H. Roark, Annu. Rev. Immunol. 15 (1997) 535–562.

[3] M. Shimamura, Y.-Y. Huang, FEBS Lett. 516 (2002) 97–100.

[4] F. Tilloy, E. Treiner, S.-H. Park, G. Garcia, F. Lemonnier, H. de la Salle, A. Bendelac, M. Bonneville, O. Lantz, J. Exp. Med. 189 (1999) 1907–1921.

[5] H. Arase, N. Arase, T. Saito, J. Exp. Med. 183 (1996) 2391–2396.

[6] T. Yoshimoto, A. Bendelac, C. Watson, J. Hu-Li, W.E. Paul, Science 270 (1995) 1845–1847.

[7] M. Shimamura, Y.-Y. Huang, K. Kobayashi, N. Okamoto, H. Goji, M. Kobayashi, Abstracts of Papers, the 2nd International Workshop on CD1 Antigen Presentation and NKT cells, Woods Hole, MA, Nov. 5–8, (2002) Abstract n° 4.

[8] N. Okamoto, O. Kanie, Y.-Y. Huang, R. Fujii, R.H. Watanabe, M. Shimamura, Chem. Biol. 12 (2005) 677–683.

[9] E. Treiner, L. Duban, S. Bahram, M. Radosavijevic, V. Wanner, F. Tilloy, P. Affaticati, S. Gilfillan, O. Lantz, Nature 422 (2003) 164–169.

[10] T. Fujita, R. Hirose, N. Hamamichi, Y. Kitao, S. Sakaki, M. Yoneta, K. Chiba, Bioorg. Med. Chem. Lett. 16 (1995) 1857–1860.

[11] M. Kiuchi, K. Adachi, T. Kohara, M. Minoguchi, T. Harano, Y. Aoki, T. Mishima, M. Arita, N. Nakao, M. Ohtsuki, Y. Hoshino, K. Teshima, K. Chiba, S. Sasaki, T. Fujita, J. Med. Chem. 43 (2000) 2946–2961.

[12] D. Kluepfel, J. Bagli, H. Baker, M.-. Charest, J. Antibiot. 25 (1972) 109–115.

[13] R. Craveri, P.L. Manachini, F. Aragozzini, Experientia 28 (1972) 867–868.

[14] V. Brinkmann, M.D. Davis, C.E. Heise, R. Albert, S. Cottents, R. Hof, C. Brunts, E. Prieschl, T. Baumruker, P. Hiestand, C.A. Foster, M. Zullinger, K.R. Lynch, J. Biol. Chem. 277 (2002) 21453–21457.

[15] S. Mandala, R. Hajdu, J. Bergstrom, E. Quackenbush, J. Xie, J. Millingan, R. Thornton, G.–. Shei, D. Card, C. Keohane, M. Rosenbach, J. Hale, C.L. Lynch, K. Rupprecht, W. Parsons, H. Rosen, H. Science 296 (2002) 346–349.

[16] T. Mukaiyama, Y. Mukai, S. Shoda, Chem. Lett. (Jpn.) (1995) 431–432.

[17] G. Eberl, R. Lees, S.T. Smiley, M. Taniguchi, M.J. Grusby, H.R. MacDonald, J. Immunol. 162 (1999) 6410–6419.

[18] T. Kawano, J. Cui, Y. Koezuka, I. Toura, Y. Kaneko, K. Motoki, H. Ueno, R. Nakagawa, H. Sato, E. Kondo, H. Koseki, M. Taniguchi, Science 278 (1999) 1626–1629.

[19] N. Burdin, L. Brossay, M. Degano, H. Iijima, M. Gui, I.A. Wilson, M. Kronenberg, Proc. Natl. Acad. Sci. USA 97 (2000) 10156–10161.

[20] R.D. Goff, Y. Gao, J. Mattner, D. Zhou, N. Yin, C. Cantu III, L. Teylon, A. Bendelac, P. Savage, J. Am. Chem. Soc. 126 (2004) 13602–13603.

[21] P. Garner, J.M. Park, J. Org. Chem. 52 (1987) 2361–2364.

[22] R. Hirose, N. Hamamichi, Y. Kitao, T. Matsuzaki, K. Chiba, T. Fujita, Bioorg. Med. Chem. Lett. 6 (1996) 2647–2650.

[23] J. Tamura, S. Horito, J. Yoshimura, H. Hashimoto, Carbohydr. Res. 207 (1990) 153–165.

[24] M. Morita, K. Motoki, K. Akimoto, T. Natori, T. Sakai, E. Sawa, K. Yajima, Y. Koezuka, E. Kobayashi, H. Fukushima, J. Med. Chem. 18 (1995) 1487–1491.

[25] T. Yoshimoto, A. Bendelac, C. Watson, J. Hu-Li, W.E. Paul, Science 270 (1995) 1845–1847.

Essential Role of IκB Kinase α in Thymic Organogenesis Required for the Establishment of Self-Tolerance[1]

Dan Kinoshita,[*] Fumiko Hirota,[‡] Tsuneyasu Kaisho,[§] Michiyuki Kasai,[¶] Keisuke Izumi,[†] Yoshimi Bando,[†] Yasuhiro Mouri,[‡] Akemi Matsushima,[‡] Shino Niki,[‡] Hongwei Han,[‡] Kiyotaka Oshikawa,[‡] Noriyuki Kuroda,[‡] Masahiko Maegawa,[*] Minoru Irahara,[*] Kiyoshi Takeda,[‖] Shizuo Akira,[#] and Mitsuru Matsumoto[2‡]

IκB kinase (IKK) α exhibits diverse biological activities through protein kinase-dependent and -independent functions, the former mediated predominantly through a noncanonical NF-κB activation pathway. The in vivo function of IKKα, however, still remains elusive. Because a natural strain of mice with mutant NF-κB-inducing kinase (NIK) manifests autoimmunity as a result of disorganized thymic structure with abnormal expression of Rel proteins in the thymic stroma, we speculated that the NIK-IKKα axis might constitute an essential step in the thymic organogenesis that is required for the establishment of self-tolerance. An autoimmune disease phenotype was induced in athymic nude mice by grafting embryonic thymus from IKKα-deficient mice. The thymic microenvironment that caused autoimmunity in an IKKα-dependent manner was associated with defective processing of NF-κB2, resulting in the impaired development of thymic epithelial cells. Thus, our results demonstrate a novel function for IKKα in thymic organogenesis for the establishment of central tolerance that depends on its protein kinase activity in cooperation with NIK. *The Journal of Immunology*, 2006, 176: 3995–4002.

T he transcription factor NF-κB plays an important role in the regulation of innate immunity, stress responses, inflammation, and the inhibition of apoptosis (1, 2). The activity of NF-κB is tightly regulated through the IκB kinase (IKK)[3] complex, which consists of two catalytic subunits (IKKα and IKKβ) and a regulatory subunit (IKKγ) (2). IKKα has been shown to be phosphorylated by NF-κB-inducing kinase (NIK) (3), which is structurally related to MEK kinase (4). Many aspects of the in vivo function of these key players have been elucidated by the use of both gene-targeted mice and natural mutant mice (2). The alymphoplasia (aly) strain of mice carries a natural mutation

of the NIK gene (5, 6) in which a G855R substitution in the C terminus of the protein results in inability to bind to IKKα (7). We have demonstrated previously that a defective NIK-IKKα axis downstream of lymphotoxin (LT) βR, a receptor essential for secondary lymphoid organogenesis (8), is responsible for the abnormal development of secondary lymphoid organs in aly mice (7, 9).

In addition to its essential role in secondary lymphoid organogenesis, we have demonstrated recently that NIK is required in the thymic stroma for the organization of the thymic microenvironment (10). Abnormal thymic organogenesis in the absence of normal NIK accounts for the autoimmune disease phenotype seen in aly mice, which is characterized by chronic inflammatory changes in several organs, including the liver, pancreas, salivary gland, and lacrimal gland (5, 10). Because breakdown of self-tolerance is considered to be the key event responsible for the autoimmune disease process, and establishment of self-tolerance primarily depends on physical contact between thymocytes and thymic stroma (11), characterization of the stromal elements involved may contribute to the development of a therapeutic approach to many autoimmune diseases.

Medullary thymic epithelial cells (mTECs) play pivotal roles in the cross talk between developing thymocytes and thymic stroma (12). Elimination of autoreactive T cells (negative selection) and/or production of immunoregulatory T cells (Tregs) are most likely mediated by a set of self Ags expressed on mTECs (13, 14). In fact, gene expression studies have demonstrated that mTECs are a specialized cell type in which promiscuous expression of a broad range of tissue-specific Ag (TSA) genes is an autonomous property (15). Studies on mice with autoimmune phenotypes resulting from an abnormal thymic microenvironment have provided useful insights into this mechanism. Autoimmune regulator (Aire)-deficient mice have mTECs with reduced expression of many, but not all, TSAs, but have apparently normal thymic structure (16, 17). These results suggest that Aire regulates transcription of TSAs within developed mTECs without influencing the development of these cells. In contrast, reduced expression of TSAs (and Aire) in the thymus from NIK mutant mice is associated with impaired development of mTECs (10); NIK[aly/aly]

mice lack *Ulex europaeus* (UEA)-1⁺ mTECs and have reduced numbers of ER-TR5⁺ mTECs. Although these results are consistent with the idea that NIK affects TSA expression in the thymus through a developmental effect on mTECs, it is not clear whether NIK has any significant roles in the transcription of TSA genes within these cells, as suggested for Aire.

Initial studies of mice deficient in IKKα have unveiled an unexpected function of IKKα for the development of limbs and skin (18, 19). Subsequent studies have revealed a two-dimensional role for IKKα, which possesses both protein kinase-dependent and protein kinase-independent functions. It has been demonstrated that kinase activity is required for lymphoid organogenesis (7, 20). B cell development and function (21), and mammary gland development (22). In contrast, kinase-independent activity is required for epidermal keratinocyte differentiation and skeletal and craniofacial morphogenesis (23, 24). Perinatal death of IKKα⁻/⁻ mice, however, has hampered a detailed analysis of the in vivo immunological function of IKKα. Given that NIK*ᵃˡʸ/ᵃˡʸ* mice have disorganized thymic structure together with an organ-specific autoimmune disease, we hypothesized that IKKα in the thymic stroma has similar roles to those of NIK. In the present study, we have examined this hypothesis and demonstrated that IKKα regulates thymic organogenesis and establishes self-tolerance primarily through a noncanonical NF-κB activation pathway with NIK, which requires the processing of NF-κB2 (i.e., production of p52 from its precursor p100) (25). With the use of isolated thymic epithelial cells (TECs) together with mTEC lines established from NIK*ᵃˡʸ/ᵃˡʸ* mice, we have also demonstrated that the NIK-IKKα axis regulates thymic expression of TSAs predominantly through the developmental process of mTECs, not through transcriptional control of TSA genes within developed mTECs. Thus, our results illustrate a novel function of IKKα in thymic stroma-dependent self-tolerance that cannot be compensated for by the related IKKβ subunit.

Materials and Methods

Mice

BALB/cA Jcl-*r* mice (BALB/c*ᶯᵘ/ᵘ* mice) and NIK*ᵃˡʸ/ᵃˡʸ* mice were purchased from CLEA Japan, and Rag2-deficient mice on BALB/c background were acquired from Taconic Farms. IKKα⁻/⁻ mice were generated by gene targeting, as described previously (18). The mice were maintained under pathogen-free conditions and were handled in accordance with the Guidelines for Animal Experimentation of Tokushima University School of Medicine.

Thymus grafting

Thymus grafting was performed, as previously described (10). Briefly, thymic lobes were isolated from embryos at 14.5 days postcoitus and were cultured for 4 days on top of Nucleopore filters (Whatman) placed on RPMI 1640 medium (Invitrogen Life Technologies) supplemented with 10% heat-inactivated FBS (Invitrogen Life Technologies). 2 mM ʟ-glutamine. 100 U/ml penicillin. 100 μg/ml streptomycin. 50 μM 2-ME, and 1.35 mM 2'-deoxyguanosine (2-DG; Sigma-Aldrich). Five pieces of thymic lobes were grafted under the renal capsule of BALB/c*ᶯᵘ/ᵘ* mice. After 6–8 wk, reconstitution of peripheral T cells was determined by flow cytometric analysis (BD Biosciences) with anti-CD4 (clone GK1.5: BD Pharmingen) and anti-CD8 (clone 53-6.7: BD Pharmingen) mAbs, and then thymic chimeras were used for the analyses.

Western blotting

Proteins extracted from embryonic thymic lobes, prepared as described above, were analyzed with an ECL Western blotting detection system (Amersham Biosciences). Rabbit anti-peptide Abs directed against p52 (catalog no. sc-298) and RelB (catalog no. sc-226), mouse anti-*Ick* mAb (catalog no. sc-433), and goat anti-actin Ab (catalog no. sc-1616) were all purchased from Santa Cruz Biotechnology.

Pathology

Formalin-fixed tissue sections were subjected to H&E staining, and two pathologists independently evaluated the histology without being informed

of the detailed condition of the individual mouse. Histological changes were scored as 0 (no change), 1 (mild lymphoid cell infiltration), or 2 (marked lymphoid cell infiltration).

Establishment of TEC lines from NIK*ᵃˡʸ/ᵃˡʸ* mice

TEC lines were established from NIK*ᵃˡʸ/ᵃˡʸ* embryos at 14.5 days postcoitus, as previously described (26). These cells were maintained with gamma ray-irradiated (40 Gy) Swiss 3T3 cells as feeder cells in calcium-free MEM (Invitrogen Life Technologies) supplemented with 10% heat-inactivated FBS, 3 mM ʟ-glutamine, 50 μg/ml gentamicin, 50 μM 2-ME, and 1 μg/ml hydrocortisone (Sigma-Aldrich). NIK*ᵃˡʸ/ᵃˡʸ* mouse origin was confirmed by sequencing of the *aly*-type NIK gene (6, 7).

Immunohistochemistry

Immunohistochemical analysis of the grafted thymus was performed, as previously described (10). Briefly, frozen tissue sections were fixed in cold acetone and stained by first incubating them with ER-TR5 (27) and UEA-1-biotin (Vector Laboratories). After being washed, the sections were further incubated with Alexa 594-conjugated goat anti-rat IgG (Invitrogen Life Technologies) and Alexa 488-conjugated streptavidin (Invitrogen Life Technologies) for the immunofluorescence. For the detection of autoantibodies, serum from thymic chimeras was incubated with various organs obtained from Rag2-deficient mice. FITC-conjugated anti-mouse IgG Ab (Southern Biotechnology Associates) was used for the detection. Polyclonal anti-Aire Ab was produced by immunizing rabbits with peptides corresponding to the COOH-terminal portion of mouse Aire, and Alexa 488-conjugated donkey anti-rabbit IgG (Invitrogen Life Technologies) was used as a secondary Ab for detection. TEC lines established from NIK*ᵃˡʸ/ᵃˡʸ* embryos were seeded on coverslips and subjected to immunohistochemistry, as previously described (28). Anti-epithelial cell adhesion molecule (Ep-CAM) mAb (BD Biosciences) and anti-keratin-5 polyclonal Ab (Covance) were used for the staining. DNA staining was with 4'6-diamidino-2-phenylindole (Roche Applied Science).

NF-κB2 processing

TECs were stimulated with agonistic anti-LTβR mAb (clone AF.H6: provided by P. Rennert, Biogen Idec) (29) (5 μg/ml) or with agonistic anti-CD40 mAb (clone 3/23; Serotec) (5 μg/ml) for 8 h. Cytoplasmic and nuclear extracts were prepared from the cells, as described previously (30), and were subjected to Western blotting with rabbit anti-p52 Ab from Upstate Biotechnology (catalogue 06-413).

Thymic stroma preparation

Thymic stroma was prepared, as described previously (17). Briefly, thymic lobes were isolated from three to six mice for each group and cut into small pieces. The fragments were gently rotated in RPMI 1640 medium (Invitrogen Life Technologies) supplemented with 10% heat-inactivated FCS (Invitrogen Life Technologies), 20 mM HEPES, 100 U/ml penicillin, 100 μg/ml streptomycin, and 50 μM 2-ME, hereafter referred to as R10, at 4°C for 30 min, and dispersed further with pipetting to remove the majority of thymocytes. The resulting thymic fragments were digested with 0.15 mg/ml collagenase IV (Sigma-Aldrich) and 10 U/ml DNase 1 (Roche Molecular Biochemicals) in RPMI 1640 at 37°C for 15 min. The supernatants that contained dissociated TECs were saved, whereas the remaining thymic fragments were further digested with collagenase IV and DNase I. This step was repeated twice, and the remaining thymic fragments were digested with collagenase IV. DNase I, and 0.1 mg/ml dispase I (Roche Applied Science) at 37°C for 30 min. The supernatants from this digest were combined with the supernatants from the collagenase digests, and the mixture was centrifuged for 5 min at 450 × *g*. The cells were suspended in PBS containing 5 mM EDTA and 0.5% FCS and kept on ice for 10 min. CD45⁻ thymic stromal cells were then purified by depleting CD45⁺ cells with MACS CD45 microbeads (Miltenyi Biotec), according to the manufacturer's instructions. The resulting preparations contained ~60% Ep-CAM⁺ cells and <10% thymocytes (i.e., CD4/CD8 single-positive and CD4/CD8 double-positive cells), as determined by flow cytometric analysis.

Real-time PCR and semiquantitative RT-PCR

Real-time PCR for quantification of TSA genes was conducted with cDNA prepared from RNAs extracted from whole thymus or from isolated TECs. The primers, the probes, and the reactions were those described previously (10, 17). Cathepsin S primers were 5'-GCCATTCCTCCTTCTTCTTC TACA-3' and 5'-CAAGAACACCATGATTCACATTGC-3', and the cathepsin S probe was 5'-FAM-AAGCGGTGTCTATGATGACCCCTCCT GTA-3' (31). Semiquantitative RT-PCR of TSA genes was conducted, as previously described (10, 17).

FIGURE 1. Unaltered thymocyte development in the absence of IKKα in fetal thymic organ culture. Thymic lobes isolated from embryos of both control (center panels) and IKKα⁻/⁻ (right panels) mice at 14.5 days post-coitus supported maturation of thymocytes similarly in a 4-day organ culture in the absence of 2-DG. Flow cytometric analysis with forward scatter (FSC) and side scatter (SSC) (top panels), and with anti-CD4 and anti-CD8 mAbs (bottom panels). Thymic organ culture of control mice in the presence of 2-DG is shown as a negative control (left panels). One representative result from a total of two repeats is shown.
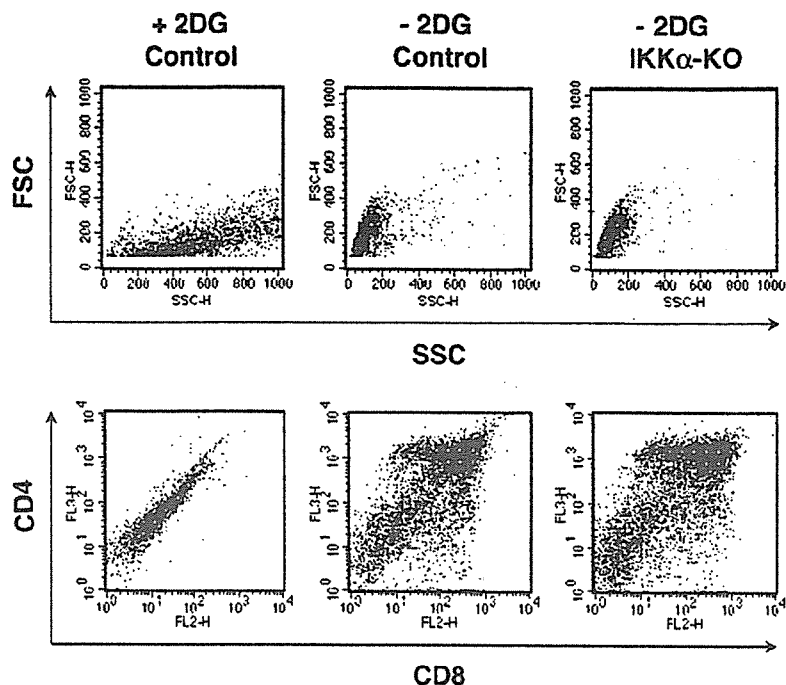
Results

IKKα in the thymic stroma is required for self-tolerance

We have demonstrated recently that aly mice, a natural strain with mutant NIK, manifest autoimmunity resulting from disorganized thymic structure with abnormal expression of Rel proteins in the thymic stroma (10). Although the identity of the upstream receptor(s) controlling NIK-dependent thymic organogenesis has not been fully determined (see Discussion), we speculated that IKKα might function as a downstream kinase of NIK in this process. Because of the perinatal death of IKKα⁻/⁻ mice (18, 19), we assessed thymic organogenesis and T cell development in IKKα⁻/⁻ mice by using embryonic thymus; thymic lobes were isolated from control and IKKα⁻/⁻ embryos at 14.5 days postcoitus and cultured for 4 days in vitro. Such thymic lobes supported maturation of thymocytes similarly in both control and IKKα⁻/⁻ mice (Fig. 1), indicating a dispensable role of IKKα in both thymocytes and thymic stroma in their developmental cross talk. The dispensability of IKKα in thymocyte development assessed with this fetal thymus organ culture system is consistent with the observation of normal T cell development in chimeras in which IKKα⁻/⁻ fetal liver cells were transferred into irradiated Rag2-deficient mice (21). Of importance, histological examination of those chimeras showed no signs of autoimmune disease (T. Kaisho, K. Izumi, and M. Matsumoto, unpublished observation), suggesting that IKKα-deficient T cells do not promote the development of autoimmune disease in a cell-autonomous manner. In contrast, we speculated that IKKα in thymic stroma might be essential for the establishment of self-tolerance, as demonstrated for NIK (10). To test this hypothesis, we generated thymic chimeras. The 2-DG-treated embryonic thymic lobes, which did not contain any live thymocytes as determined by flow cytometric analysis (see Fig. 1, left panels) and by Western blotting with anti-lck Ab (see Fig. 2, top panel), were prepared and then grafted under the renal capsule of BALB/c^{nu/nu} mice. In this system, mature T cells derived from IKKα-sufficient recipient BALB/c^{nu/nu} mouse bone marrow are produced de novo through interaction with the grafted thymic stroma. Grafting both control and IKKα⁻/⁻ embryonic thymus induced T cell maturation in the periphery of BALB/c^{nu/nu} mice to a similar extent: CD4⁺ T cells plus CD8⁺ T cells were

14.1 ± 5.3% in BALB/c^{nu/nu} mice grafted with control thymus (n = 6) compared with 15.1 ± 7.6% in BALB/c^{nu/nu} mice grafted with IKKα⁻/⁻ thymus (n = 7). Remarkably, histological examination of IKKα⁻/⁻ thymus-grafted mice, but not control thymus-grafted mice, revealed many lymphoid cell infiltrations in the liver, mainly in the portal area (Fig. 3, A and B), which is reminiscent of the autoimmune disease phenotype observed in NIK^{aly/aly} mice. To see whether T cells developed in a thymic microenvironment without IKKα in those mice are autoreactive per se, we injected splenocytes obtained from BALB/
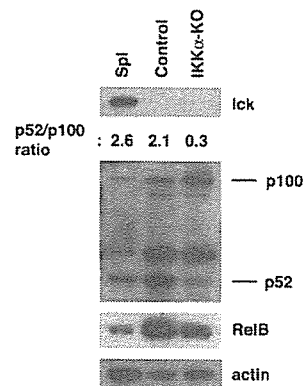
FIGURE 2. IKKα regulates the processing of NF-κB2 in thymic stroma. Thymic lobes isolated from control (second lane) and IKKα⁻/⁻ embryos (third lane), and cultured for 4 days in the presence of 2-DG contain no live thymocytes, as demonstrated by the lack of lck expression with Western blotting (top panel). The same blot was probed with anti-Rel protein Abs (two middle panels) and anti-actin Ab (bottom panel). p52 processing from the precursor p100 was impaired in thymic stroma from IKKα⁻/⁻ mice. RelB expression was also reduced in IKKα⁻/⁻ thymus. Total splenocytes (Spl) from wild-type mice were used as control (first lane). Intensities of the bands of p100 and p52 in each lane were measured with ImageJ software (National Institutes of Health), and the ratios between p52 and p100 are shown above the NF-κB2 Western blot. One representative result from a total of three repeats is shown.
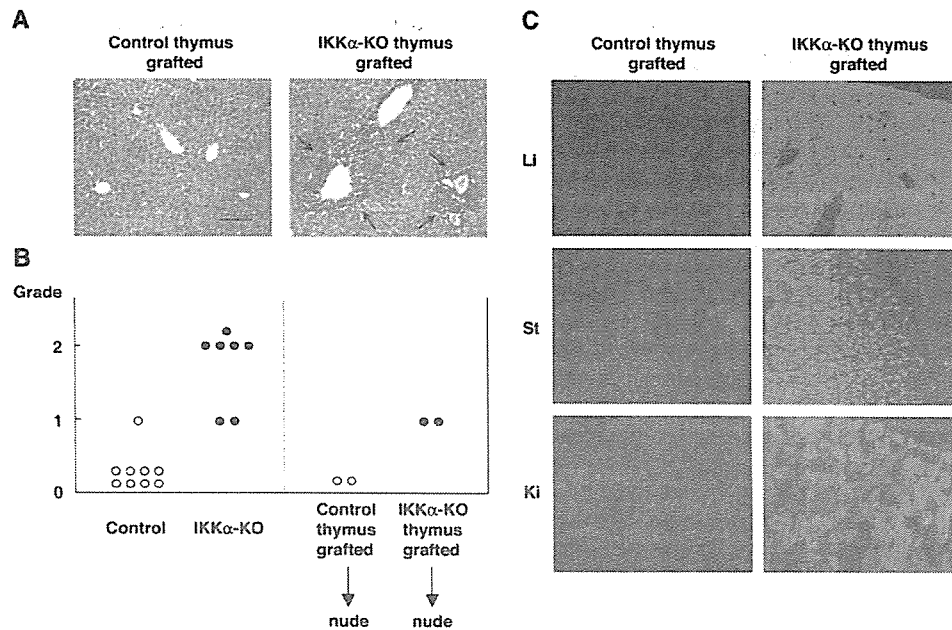
FIGURE 3. Requirement for IKKα in thymic stroma for the establishment of self-tolerance. *A*. BALB/c$^{nu/nu}$ mice grafted with IKKα$^{-/-}$ embryonic thymus (*right panel*), but not with control embryonic thymus (*left panel*), developed an autoimmune disease phenotype in the liver. Arrows indicate the lymphoid cell infiltrations. The scale bar corresponds to 100 μm in size. *B*. Many IKKα$^{-/-}$ thymus-grafted BALB/c$^{nu/nu}$ mice exhibited lymphoid cell infiltrations in the liver (●; *left half panel*). In contrast, these changes were scarcely observed in control thymus-grafted mice (○). Injection of splenocytes obtained from BALB/c$^{nu/nu}$ mice grafted with IKKα-deficient thymus into another group of BALB/c$^{nu/nu}$ mice induced lymphoid cell infiltration in the liver of the recipient mice (●; *right half panel*), whereas injection of splenocytes obtained from BALB/c$^{nu/nu}$ mice grafted with control thymus induced no such changes in the recipient mice (○). Histological changes in H&E-stained tissue sections were scored as 0 (no change), 1 (mild lymphoid cell infiltration), or 2 (marked lymphoid cell infiltration). One mark corresponds to one mouse analyzed. *C*. Serum from BALB/c$^{nu/nu}$ mice grafted with IKKα$^{-/-}$ thymus (*right panels*), but not with control thymus (*left panels*), contained IgG class autoantibodies against liver (Li: *top panels*), stomach (St: *middle panels*), and kidney (Ki: *bottom panels*) detected with immunofluorescence. Original magnification. ×100.

---

c$^{nu/nu}$ mice grafted with IKKα-deficient thymus into another group of BALB/c$^{nu/nu}$ mice. We observed similar lymphoid cell infiltration in the liver of the recipient mice, whereas injection of splenocytes obtained from BALB/c$^{nu/nu}$ mice grafted with control thymus induced no such changes in the recipients (Fig. 3*B*). These results clearly indicate the significance of IKKα as a thymic stromal element required for the establishment of self-tolerance. Five of seven IKKα$^{-/-}$ thymus-grafted mice also showed lymphoid cell infiltrations in the pancreas (perivascular areas near islets), although these infiltrations were less marked than in the liver (D. Kinoshita, K. Izumi, and M. Matsumoto, unpublished observation).

Development of autoimmunity in athymic *nude* mice grafted with IKKα$^{-/-}$ thymus was further demonstrated by the production of autoantibodies against various organs. When the serum from BALB/c$^{nu/nu}$ mice grafted with IKKα$^{-/-}$ thymus was tested for reactivity against liver, six of seven showed IgG class autoantibodies as detected with immunofluorescence (Fig. 3*C*). In contrast, such activity was observed in only one of six control thymus-grafted mice, and this activity was only weak. Similarly, high incidences of autoantibodies against stomach (five of seven) and kidney (six of seven) were observed in IKKα$^{-/-}$ thymus-grafted mice, although on histological examination these organs appeared unaffected when assessed 6–8 wk after thymus graft (D. Kinoshita, K. Izumi, and M. Matsumoto, unpublished observation).

IKKα in the thymic stroma regulates Rel protein expression and thymic organogenesis

Given that IKKα plays an essential role in the thymic microenvironment that is required for the establishment of self-tolerance, we investigated the expression of Rel proteins from IKKα$^{-/-}$ thymic stroma by Western blotting. Thymic lobes used for this experiment were isolated from control and IKKα$^{-/-}$ embryos at 14.5 days postcoitus and treated with 2-DG to isolate only thymic stromal elements, as described above. Expression of p52 was significantly reduced in the thymic stroma from IKKα$^{-/-}$ mice compared with that from control mice, whereas p100, a precursor form of p52, was more abundant in IKKα$^{-/-}$ mice than in control mice (Fig. 2): the amount of p52 in thymic stroma from control mice was double that of p100, whereas the ratio of p52 to p100 was reversed in IKKα$^{-/-}$ mice. Thus, IKKα-dependent generation of p52 from p100 in thymic stroma might constitute a second NF-κB signaling pathway, as we originally observed in hemopoietic cells (32) and subsequently characterized for signals through LTβR (33), CD40 (34), and B cell activating factor of the TNF family receptor (35, 36). RelB expression in the thymic stroma was slightly reduced in IKKα$^{-/-}$ mice compared with that in control mice (Fig. 2), as observed in NIK$^{aly/aly}$ mice (10). These results suggest that the disturbed thymic microenvironment in IKKα$^{-/-}$ mice is associated with abnormal regulation of the NF-κB activation pathway in the thymic stroma in the absence of IKKα.

The essential roles of IKKα in thymic stroma were also confirmed by histological examination of the grafted thymus. Although embryonic thymus from control mice that had been grafted onto BALB/c$^{nu/nu}$ mice contained mTECs that bound with UEA-1, IKKα$^{-/-}$ embryonic thymus grafted onto BALB/c$^{nu/nu}$ mice did not have UEA-1$^+$ cells (Fig. 4*A*). ER-TR5$^+$ mTECs were sparse in IKKα$^{-/-}$ embryonic thymus grafted onto BALB/c$^{nu/nu}$ mice compared with control embryonic thymus grafted similarly (Fig. 4*A*). Abnormal development of mTECs in the absence of IKKα

A

| ER-TR5 | UEA-1 | Merge |

B

Control thymus grafted   IKKα-KO thymus grafted

aly/+   aly/aly
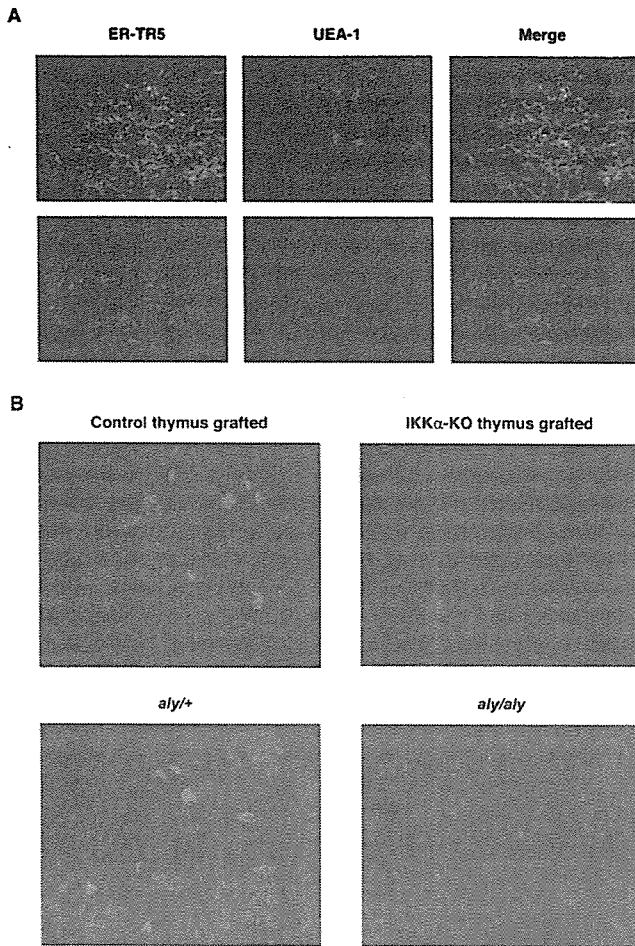
FIGURE 4. IKKα is required for thymic organization. *A*. Embryonic thymus from IKKα$^{-/-}$ mice contained no UEA-1$^+$ cells (*bottom middle panel*) and fewer ER-TR5$^+$ medullary epithelial cells stained in red (*bottom left panel*) after grafting onto BALB/c$^{nu/nu}$ mice compared with that from control mice (*top left panel*). UEA-1$^+$ cells from control embryonic thymus grafted onto BALB/c$^{nu/nu}$ mice were stained in green (*top middle panel*), and were merged with ER-TR5 staining (*top right panel*). *B*. Embryonic thymus from IKKα$^{-/-}$ mice grafted onto BALB/c$^{nu/nu}$ mice contained very few Aire$^+$ cells (*top right panel*), as observed in adult untreated NIK$^{aly/aly}$ thymus (*bottom right panel*). Aire$^+$ cells were observed in embryonic thymus from control mice grafted onto BALB/c$^{nu/nu}$ mice (*top left panel*) and adult untreated NIK$^{aly/+}$ thymus (*bottom left panel*). Original magnification. ×200. One representative result from a total of five repeats is shown.

was also exemplified by the loss of Aire$^+$ cells in IKKα$^{-/-}$ embryonic thymus grafted onto BALB/c$^{nu/nu}$ mice (Fig. 4*B*). A dramatic decrease in the number of Aire$^+$ cells was also observed in adult untreated NIK$^{aly/aly}$ thymus (Fig. 4*B*). Because T cells with

normal IKKα (derived from BALB/c$^{nu/nu}$ mice) cannot restore normal mTECs in the IKKα$^{-/-}$ thymus when the interaction between T cells and thymic stromal cells is initiated from the embryonic stage, the contribution of IKKα to thymic organogenesis seems to be stromal element autonomous. These results clearly indicate indispensable roles for IKKα as a stromal element in the thymic organogenesis that is required for the establishment of self-tolerance.

Developmental effect of NIK for promiscuous gene expression in the thymus

Promiscuous gene expression of many TSAs in mTECs could play an essential role in the establishment of central tolerance (12). The autoimmunity developed in NIK$^{aly/aly}$ mice (10) and IKKα$^{-/-}$ mice, described above, might be associated with altered expression of self Ags in the thymus. In fact, NIK$^{aly/aly}$ thymus showed dramatically reduced transcription of many TSAs (10). We have examined whether thymic expression of TSAs is influenced by the absence of IKKα using embryonic thymus grafted onto BALB/c$^{nu/nu}$ mice: RNAs were extracted from the thymus 6 wk after grafting when the thymus was colonized with developing thymocytes derived from BALB/c$^{nu/nu}$ mouse bone marrow. By real-time PCR. salivary protein 1 (SP1). fatty acid-binding protein (FABP). C-reactive protein (CRP). and glutamic acid decarboxylase 67 (GAD67) were easily detected in grafted control thymus. whereas expression of SP1. FABP. and GAD67 was below the limit of detection in grafted IKKα$^{-/-}$ thymus. Although CRP was detected in grafted IKKα$^{-/-}$ thymus (N. Kuroda and M. Matsumoto, unpublished observation). its expression was reduced: the value for CRP/hypoxanthine phosphoribosyltransferase (HPRT) from control thymus was 1.61, and that for CRP/HPRT from IKKα$^{-/-}$ thymus was 0.32.

Because we used RNAs extracted from total thymus instead of isolated mTECs in both previous experiments with NIK$^{aly/aly}$ mice (10) and experiments with IKKα$^{-/-}$ thymic chimeras described above. it is not clear whether reduced expression of TSAs was due to the reduced number of mTECs expressing TSAs (15) or to the lack of NIK-IKKα-dependent transcriptional control of TSA genes. To test these possibilities. we harvested TECs (which contain both cortical and medullary components) from adult NIK$^{aly/aly}$ mice and examined the expression of TSAs together with cathepsin S (CAT-S). which is highly expressed by mTECs in the thymic stroma (31). Consistent with immunohistochemical evaluation demonstrating less abundant mTECs in NIK$^{aly/aly}$ mice (10), TECs purified from NIK$^{aly/aly}$ thymus showed reduced expression of CAT-S (Table I): the ratio between the values from NIK$^{aly/+}$ mice and NIK$^{aly/aly}$ mice was 0.12. When RNAs extracted from purified TECs were tested for TSA expression by real-time PCR using HPRT as an internal control. the difference between NIK$^{aly/+}$ and NIK$^{aly/aly}$ mice became subtle when compared with the results obtained from total thymus. except for CRP (Table I). This

Table I. *Expression of tissue-specific genes in the thymus[a]*

Genotype	SP1	FABP	CRP	GAD67	CAT-S
aly/+	7.97/6.28	6.10/7.62	1.30/3.04	7.18/3.80	N.A./12.2[b]
aly/aly	7.45 × 10^{-2}/18.2	4.08 × 10^{-1}/0.21	9.49 × 10^{-2}/0.14	4.44 × 10^{-2}/0.64	N.A./1.44
Relative abundance[c] (aly/aly vs aly/+)	0.93 × 10^{-2}/2.90	0.67 × 10^{-2}/0.03	0.07/0.05	0.62 × 10^{-2}/0.17	N.A./0.12

[a] Real-time PCR for peripheral tissue-specific genes (i.e.. *SP1. FABP. CRP. GAD67.* and *CAT-S*) was performed using RNAs extracted from total thymus (shown on the left) or RNAs extracted from purified TECs (shown on the right) from NIK$^{aly/+}$ and NIK$^{aly/aly}$ mice. *Hprt* expression level was used as an internal control. Pools of TECs isolated from three to six mice of each group were used for the analysis. One representative result from a total of two repeats is shown.

[b] N.A.. Not applicable.

[c] The relative abundance of each gene was calculated from the ratio between the values from NIK$^{aly/+}$ mice and NIK$^{aly/aly}$ mice (e.g.. the *SP1/Hprt* value from NIK$^{aly/aly}$ mice was divided by the *SP1/Hprt* value from NIK$^{aly/+}$ mice).

finding is more obvious when taking into account that TECs purified from NIK$^{aly/aly}$ thymus contained reduced mTEC components compared with those from NIK$^{aly/+}$ thymus, as revealed by the reduced expression of CAT-S. These results suggest that NIK regulates thymic expression of TSAs predominantly through the developmental process of mTECs, and not through transcriptional control of TSA genes within developed mTECs.

To further confirm this finding, we used mTEC lines established from the thymus. Because we were not able to establish TEC lines from IKKα$^{-/-}$ embryos at 18.5 days postcoitus for unknown reasons, we used mTEC lines established from NIK$^{aly/aly}$ embryos for this purpose: it is possible that the protein kinase-independent function of IKKα may contribute to the growth disadvantage of TECs lacking IKKα (23, 24). We established three cell lines from NIK$^{aly/aly}$ embryonic thymus (5-1, 4-1-3, and 6-5T), and these cells were positive for Ep-CAM, an epithelial cell marker, and staining with keratin-5 and ER-TR5 (Fig. 5A), but negative for keratin-8 and Th-3 (Ref. 26 and Y. Mouri, M. Kasai, and M. Matsumoto, unpublished observation), consistent with a medullary origin. The TEC origin of these lines was also verified by Foxn1 expression (Fig. 5C). In these NIK$^{aly/aly}$ mTECs, agonistic stimulation of LTβR by mAb AF.H6 (29) did not induce NF-κB2 processing, in contrast to the mTECs derived from wild-type C57BL/6 mice (26) (Fig. 5B): LTβR ligation on wild-type mTEC increased amount of p52 in the nucleus (Nucl: bottom panel) with a concomitant reduction of p100 in the cytoplasm (Cyto: top panel),

whereas the same treatment induced no nuclear p52 in NIK$^{aly/aly}$ mTEC. In contrast, CD40 ligation on both wild-type and NIK$^{aly/aly}$ mTECs had no such effect, which is consistent with the fact that CD40$^{-/-}$ mice showed undisturbed thymic architecture with normal distribution of mTECs containing UEA-1$^+$ cells, ER-TR5$^+$ cells, and Aire$^+$ cells (Y. Mouri and M. Matsumoto, unpublished observation). Thus, these established cell lines show many of the characteristics of mTECs while retaining the features of aly-type NIK mutation.

mTEC lines established from NIK$^{aly/aly}$ mice showed levels of TSAs that were indistinguishable from those of control mTECs (Fig. 5C): SP1 and FABP were expressed from all the lines from both wild-type and NIK$^{aly/aly}$ mTECs. Expression of CRP assessed with real-time PCR was also indistinguishable between wild-type and NIK$^{aly/aly}$ mTECs: CRP/HPRT values from wild-type mTECs were 4.93 (line 2-3), 1.04 (line 1C6), and 2.21 (line 3-10), and CRP/HPRT values from NIK$^{aly/aly}$ mTECs were 2.75 (line 5-1), 1.67 (line 4-1-3), and 3.01 (line 6-5T). Insulin/HPRT values from wild-type mTECs were 0.47 (line 1C6) and 1.66 (line 3-10), and insulin/HPRT values from NIK$^{aly/aly}$ mTECs were 0.50 (line 5-1), 0.33 (line 4-1-3), and 0.65 (line 6-5T). Taken together, these results suggest that NIK is not required in individual mTECs for the transcriptional control of TSA genes. Rather, reduced expression of TSAs in NIK$^{aly/aly}$ thymus is most likely due to the developmental effect of mutated NIK on mTECs, leading to reduced absolute numbers of mTECs, each expressing normal levels of TSAs.

FIGURE 5. Retained expression of TSA genes in mTEC lines established from NIK$^{aly/aly}$ thymus. A. TEC lines established from NIK$^{aly/aly}$ embryos (5-1, 4-1-3, and 6-5T) were positive for Ep-CAM (top panels, stained in red), keratin-5 (middle panels, stained in green), and ER-TR5 (bottom panels, stained in red). Mouse embryonic fibroblasts (MEF) served as negative control. DNA staining is with 4'6-diamidino-2-phenylindole (stained in blue). Original magnification, ×200. B. In wild-type mTEC (1C6), but not in NIK$^{aly/aly}$ mTEC (6-5T). LTβR ligation with agonistic anti-LTβR mAb increased amount of nuclear p52 (Nucl: bottom panel) with a concomitant reduction of p100 in the cytoplasm (Cyto: top panel). Such effect was observed in neither wild-type nor NIK$^{aly/aly}$ mTECs upon CD40 stimulation. One representative result from a total of three repeats is shown. Asterisks denote nonspecific bands. C. Semiquantitative RT-PCR for peripheral tissue-specific genes (SP1; FABP) was performed using mTECs established from control and NIK$^{aly/aly}$ thymus. The TEC origin of these cell lines was verified by Foxn1 expression. β-actin was used to verify equal amounts of RNAs in each sample. One representative result from a total of three repeats is shown. Asterisks denote nonspecific bands. -, Without template.
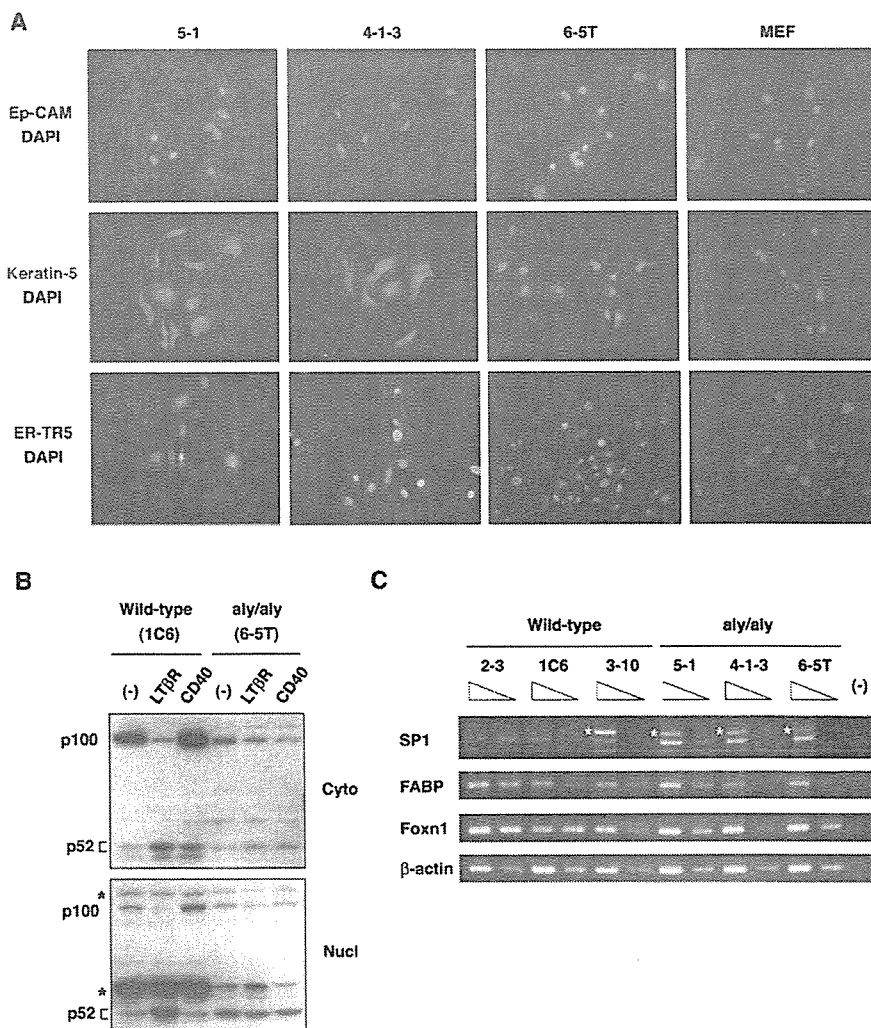
Based on the similarity of autoimmune phenotypes between NI-K$^{aly/aly}$ thymus and IKK$\alpha^{-/-}$ thymus, we speculate that IKKα regulates TSA expression in the thymus through a developmental effect similar to that of NIK.

Discussion

We have demonstrated that IKKα plays an essential role in the organization of the thymic microenvironment that is required for the establishment of central tolerance. Grafting the thymic stroma from IKK$\alpha^{-/-}$ mice onto athymic *nude* mice led to the development of autoimmune disease in the recipients: this also occurred in another group of recipient mice when the splenocytes from the IKK$\alpha^{-/-}$ thymus-grafted mice were transferred. The thymic microenvironment that caused autoimmune disease in an IKKα-dependent manner was associated with structural abnormality (lack of UEA-1$^+$ cells, and sparse ER-TR5$^+$ and Aire$^+$ cells in the medulla), defective NF-κB2 activation (impaired processing of p100 into p52), and reduced expression of TSAs. Because those phenotypes were similarly observed in NIK$^{aly/aly}$ mice (10), it is reasonable to speculate that the NIK-IKKα axis constitutes an essential step in this action, as demonstrated for secondary lymphoid organogenesis through LTβR involving NF-κB2 processing (7, 20, 37).

We have suggested that impaired processing of p100 into p52 caused by mutated NIK (10) or a lack of IKKα, as demonstrated in the present study, is relevant to the developmental defect of the thymic microenvironment. This reasoning is apparently inconsistent with the fact that mice deficient for p52 show no major defect in the thymus (38, 39). We interpret this discrepancy as a dominant effect of p100 on NF-κB activation in thymic stroma: accumulation of p100, rather than absence of p52, might be responsible for the thymic phenotypes we observed. In fact, mice lacking the COOH-terminal ankyrin domain of NF-κB2 (i.e., p100), but still containing a functional p52 protein, show abnormal development of the thymus (40), indicating the relevance of p100 to the control of thymic organogenesis. Notably, the mice deficient for p52 described above lack the whole NF-κB2 protein (including p100) because of the targeted deletion of the NF-κB2 gene locus (38, 39). We therefore consider that the ratio between p100 and p52 is a critical determinant for proper activation of the NF-κB complex that contains RelB as a heterodimeric partner (see below). Accumulation of p100 could disturb the nuclear localization of activated NF-κB complex within mTECs.

Although the exact mechanism by which IKKα regulates the thymic microenvironment that is required for the establishment of central tolerance is unknown, the existence of disorganized thymic structure together with an autoimmune disease phenotype in mice with a mutation disrupting the RelB gene merits attention. Because of the phenotypic similarities between NIK mutant mice and RelB$^{-/-}$ mice (41) (multi-inflammatory lesions together with the absence of UEA-1$^+$ mTECs), together with the roles of IKKα demonstrated in the present study, we speculate that NIK-IKKα regulates the thymic microenvironment through activation of the NF-κB complex containing RelB. A requirement for NIK for activation of the NF-κB complex containing RelB is also seen in the production of NK T cells (41, 42). Interestingly, TNFR-associated factor 6 (TRAF6) in TECs is a critical component that regulates RelB expression, thereby controlling the thymic microenvironment for the establishment of central tolerance (43). Although both NIK-IKKα-dependent and TRAF6-dependent signals merge at the level of the NF-κB complex (i.e., p52/RelB), it is reasonable to speculate that the upstream receptors of each signal are distinct, because many NIK-IKKα-dependent signals are TRAF6 independent, as exemplified for LTβR (43), and vice versa. These results suggest the existence of a group of receptor-mediated signals that

together control thymic organogenesis. The mechanisms that control the specificity of the heterodimeric complex of Rel family members (e.g., p52/RelB or p50/RelA) according to cell type and/or cellular signals also need to be clarified by future studies.

Signaling through LTβR has been demonstrated recently to control thymic organogenesis (44). However, because NIK$^{aly/aly}$ mice show more severe phenotypes of thymic structure than do LTβR-deficient mice (44), it would be reasonable to speculate that the NIK-IKKα axis is acting downstream of additional receptor(s) beyond LTβR in thymic organogenesis. Because CD40 is expressed on TECs (45, 46), and NF-κB2 processing takes place downstream of CD40, at least in B cells (34), CD40 could be a good candidate for an additional receptor that acts in NIK-IKKα-dependent thymic organogenesis. However, CD40$^{-/-}$ mice showed undisturbed thymic architecture with normal distribution of mTECs containing UEA-1$^+$ cells, ER-TR5$^+$ cells, and Aire$^-$ cells (Y. Mouri and M. Matsumoto, unpublished observation), suggesting that CD40 alone is not responsible for this action. Consistent with this finding, CD40 ligation on wild-type mTEC (and NIK$^{aly/aly}$ mTEC as well) induced no NF-κB2 processing (Fig. 5B), although flow cytometric analysis clearly demonstrated CD40 expression on both mTEC lines (S. Niki and M. Matsumoto, unpublished observation). A complete description of the upstream receptor(s) required for thymic organogenesis in a NIK-IKKα-dependent manner is essential for a better understanding of the roles of NF-κB in the establishment of central tolerance.

The cellular mechanism controlling the establishment of self-tolerance in an IKKα-dependent manner is of considerable interest. Because of the perinatal death of IKK$\alpha^{-/-}$ mice, we have investigated most of the IKKα-dependent autoimmune disease process with thymic chimeras. Because the autoimmune disease phenotype in NIK$^{aly/aly}$ mice is a result of both impaired elimination of autoreactive T cells and impaired production of Tregs (10), we suggest similar mechanisms for the breakdown of self-tolerance in the thymic microenvironment lacking IKKα. Consistent with this hypothesis, when control thymus and IKK$\alpha^{-/-}$ thymus were grafted simultaneously onto BALB/c$^{nu/nu}$ mice, the development of inflammatory lesions was not completely inhibited (D. Kinoshita, K. Izumi, and M. Matsumoto, unpublished observation), suggesting that the grafted IKK$\alpha^{-/-}$ thymus allows production of more pathogenic autoreactive T cells in the recipient mice than can be controlled by the Tregs that are produced by the grafted control thymus. We speculate that thymic stroma that has developed in the absence of IKKα may not be able to present TCR ligands (most likely containing self peptides) efficiently enough, resulting in insufficient avidity for the elimination of autoreactive T cells and/or production of Tregs (13, 14).

The autoimmunity that developed in NIK$^{aly/aly}$ mice (10) and IKK$\alpha^{-/-}$ mice, described in the present study, was associated with altered expression of self Ags in the thymus, although the significance of this finding requires further study. We investigated whether reduced expression of self Ags in a NIK-IKKα-dependent manner was due to a reduction in the number of mTECs expressing these Ags or a lack of TSA gene transcription in these cells. Because purified TECs from NIK$^{aly/aly}$ thymus largely restored TSA expression, and the levels of TSAs expressed by mTEC lines isolated from NIK$^{aly/aly}$ mice were indistinguishable from the levels expressed by wild-type mTEC lines, the reduced TSA expression by total NIK$^{aly/aly}$ thymus is most likely due to the effect of the NIK-IKKα axis on the development of mTECs. Consistent with this finding, sorted TECs from LTβR-deficient mice (which have thymic disorganization and absolute reduction of TEC number) demonstrated unaltered expression of TSA genes (44). In contrast, Aire affects TSA expression without any obvious structural abnormalities of the thymus (16, 17). Thus, TSA expression in mTECs

is controlled by a group of genes through their unique actions. Identification of particular cell types responsible for TSA expression, together with the nature of the TCR ligands (possibly TSA gene products) required for the establishment of self-tolerance, awaits further study. With the advent of thymic organogenesis using thymic precursor cells (47, 48), it may be feasible to manipulate the thymic microenvironment through the modulation of NF-κB activation pathways, thereby controlling the processes for the establishment of self-tolerance.

Acknowledgments

Disclosures

The authors have no financial conflict of interest.

References

1. Li, Q., and I. M. Verma. 2002. NF-κB regulation in the immune system. *Nat. Rev. Immunol.* 2: 725–734.

2. Karin, M., and A. Lin. 2002. NF-κB at the crossroads of life and death. *Nat. Immunol.* 3: 221–227.

3. Ling, L., Z. Cao, and D. V. Goeddel. 1998. NF-κB-inducing kinase activates IKK-α by phosphorylation of Ser-176. *Proc. Natl. Acad. Sci. USA* 95: 3792–3797.

4. Malinin, N. L., M. P. Boldin, A. V. Kovalenko, and D. Wallach. 1997. MAP3K-related kinase involved in NF-κB induction by TNF, CD95 and IL-1. *Nature* 385: 540–544.

5. Miyawaki, S., Y. Nakamura, H. Suzuka, M. Koba, R. Yasumizu, S. Ikehara, and Y. Shibata. 1994. A new mutation, *aly*, that induces a generalized lack of lymph nodes accompanied by immunodeficiency in mice. *Eur. J. Immunol.* 24: 429–434.

6. Shinkura, R., K. Kitada, F. Matsuda, K. Tashiro, K. Ikuta, M. Suzuki, K. Kogishi, T. Serikawa, and T. Honjo. 1999. Alymphoplasia is caused by a point mutation in the mouse gene encoding NF-κB-inducing kinase. *Nat. Genet.* 22: 74–77.

7. Matsushima, A., T. Kaisho, P. D. Rennert, H. Nakano, K. Kurosawa, D. Uchida, K. Takeda, S. Akira, and M. Matsumoto. 2001. Essential role of nuclear factor (NF)-κB-inducing kinase and inhibitor of κB (IκB) kinase α in NF-κB activation through lymphotoxin β receptor, but not through tumor necrosis factor receptor I. *J. Exp. Med.* 193: 631–636.

8. Matsumoto, M. 1999. Role of TNF ligand and receptor family in the lymphoid organogenesis defined by gene targeting. *J. Med. Invest.* 46: 141–150.

9. Matsumoto, M., K. Iwamasa, P. D. Rennert, T. Yamada, R. Suzuki, A. Matsushima, M. Okabe, S. Fujita, and M. Yokoyama. 1999. Involvement of distinct cellular compartments in the abnormal lymphoid organogenesis in lymphotoxin-α-deficient mice and alymphoplasia (*aly*) mice defined by the chimeric analysis. *J. Immunol.* 163: 1584–1591.

10. Kajiura, F., S. Sun, T. Nomura, K. Izumi, T. Ueno, Y. Bando, N. Kuroda, H. Han, Y. Li, A. Matsushima, et al. 2004. NF-κB-inducing kinase establishes self-tolerance in a thymic stroma-dependent manner. *J. Immunol.* 172: 2067–2075.

11. von Boehmer, H., I. Aifantis, F. Gounari, O. Azogui, L. Haughn, I. Apostolou, E. Jaeckel, F. Grassi, and L. Klein. 2003. Thymic selection revisited: how essential is it? *Immunol. Rev.* 191: 62–78.

12. Kyewski, B., and J. Derbinski. 2004. Self-representation in the thymus: an extended view. *Nat. Rev. Immunol.* 4: 688–698.

13. Shevach, E. M. 2002. CD4⁺CD25⁺ suppressor T cells: more questions than answers. *Nat. Rev. Immunol.* 2: 389–400.

14. Sakaguchi, S. 2004. Naturally arising CD4⁺ regulatory T cells for immunologic self-tolerance and negative control of immune responses. *Annu. Rev. Immunol.* 22: 531–562.

15. Derbinski, J., A. Schulte, B. Kyewski, and L. Klein. 2001. Promiscuous gene expression in medullary thymic epithelial cells mirrors the peripheral self. *Nat. Immunol.* 2: 1032–1039.

16. Anderson, M. S., E. S. Venanzi, L. Klein, Z. Chen, S. Berzins, S. J. Turley, H. Von Boehmer, R. Bronson, A. Dierich, C. Benoist, and D. Mathis. 2002. Projection of an immunological self-shadow within the thymus by the Aire protein. *Science* 298: 1395–1401.

17. Kuroda, N., T. Mitani, N. Takeda, N. Ishimaru, R. Arakaki, Y. Hayashi, Y. Bando, K. Izumi, T. Takahashi, T. Nomura, et al. 2005. Development of autoimmunity against transcriptionally unrepressed target antigen in the thymus of Aire-deficient mice. *J. Immunol.* 174: 1862–1870.

18. Takeda, K., O. Takeuchi, T. Tsujimura, S. Itami, O. Adachi, T. Kawai, H. Sanjo, K. Yoshikawa, N. Terada, and S. Akira. 1999. Limb and skin abnormalities in mice lacking IKKα. *Science* 284: 313–316.

19. Hu, Y., V. Baud, M. Delhase, P. Zhang, T. Deerinck, M. Ellisman, R. Johnson, and M. Karin. 1999. Abnormal morphogenesis but intact IKK activation in mice lacking the IKKα subunit of IκB kinase. *Science* 284: 316–320.

20. Senftleben, U., Y. Cao, G. Xiao, F. R. Greten, G. Krahn, G. Bonizzi, Y. Chen, Y. Hu, A. Fong, S. C. Sun, and M. Karin. 2001. Activation by IKKα of a second, evolutionary conserved, NF-κB signaling pathway. *Science* 293: 1495–1499.

21. Kaisho, T., K. Takeda, T. Tsujimura, T. Kawai, F. Nomura, N. Terada, and S. Akira. 2001. IκB kinase α is essential for mature B cell development and function. *J. Exp. Med.* 193: 417–426.

22. Cao, Y., G. Bonizzi, T. N. Seagroves, F. R. Greten, R. Johnson, E. V. Schmidt, and M. Karin. 2001. IKKα provides an essential link between RANK signaling and cyclin D1 expression during mammary gland development. *Cell* 107: 763–775.

23. Hu, Y., V. Baud, T. Oga, K. I. Kim, K. Yoshida, and M. Karin. 2001. IKKα controls formation of the epidermis independently of NF-κB. *Nature* 410: 710–714.

24. Sil, A. K., S. Maeda, Y. Sano, D. R. Roop, and M. Karin. 2004. IκB kinase-α acts in the epidermis to control skeletal and craniofacial morphogenesis. *Nature* 428: 660–664.

25. Pomerantz, J. L., and D. Baltimore. 2002. Two pathways to NF-κB. *Mol. Cell* 10: 693–695.

26. Kasai, M., and K. Hirokawa. 1991. A novel cofactor produced by a thymic epithelial cell line: promotion of proliferation of immature thymic lymphocytes by the presence of interleukin-1 and various mitogens. *Cell. Immunol.* 132: 377–390.

27. van Vliet, E., M. Melis, and W. van Ewijk. 1984. Monoclonal antibodies to stromal cell types of the mouse thymus. *Eur. J. Immunol.* 14: 524–529.

28. Akiyoshi, H., S. Hatakeyama, J. Pitkanen, Y. Mouri, V. Doucas, J. Kudoh, K. Tsurugaya, D. Uchida, A. Matsushima, K. Oshikawa, et al. 2004. Subcellular expression of autoimmune regulator (AIRE) is organized in a spatiotemporal manner. *J. Biol. Chem.* 279: 33984–33991.

29. Rennert, P. D., D. James, F. Mackay, J. L. Browning, and P. S. Hochman. 1998. Lymph node genesis is induced by signaling through the lymphotoxin β receptor. *Immunity* 9: 71–79.

30. Matsumoto, M., T. Yamada, S. K. Yoshinaga, T. Boone, T. Horan, S. Fujita, Y. Li, and T. Mitani. 2002. Essential role of NF-κB-inducing kinase in T cell activation through the TCR/CD3 pathway. *J. Immunol.* 169: 1151–1158.

31. Gallegos, A. M., and M. J. Bevan. 2004. Central tolerance to tissue-specific antigens mediated by direct and indirect antigen presentation. *J. Exp. Med.* 200: 1039–1049.

32. Yamada, T., T. Mitani, K. Yorita, D. Uchida, A. Matsushima, K. Iwamasa, S. Fujita, and M. Matsumoto. 2000. Abnormal immune function of hemopoietic cells from alymphoplasia (*aly*) mice, a natural strain with mutant NF-κB-inducing kinase. *J. Immunol.* 165: 804–812.

33. Xiao, G., E. W. Harhaj, and S. C. Sun. 2001. NF-κB-inducing kinase regulates the processing of NF-κB2 p100. *Mol. Cell* 7: 401–409.

34. Coope, H. J., P. G. Atkinson, B. Huhse, M. Belich, J. Janzen, M. J. Holman, G. G. Klaus, L. H. Johnston, and S. C. Ley. 2002. CD40 regulates the processing of NF-κB2 p100 to p52. *EMBO J.* 21: 5375–5385.

35. Kayagaki, N., M. Yan, D. Seshasayee, H. Wang, W. Lee, D. M. French, I. S. Grewal, A. G. Cochran, N. C. Gordon, J. Yin, et al. 2002. BAFF/BLyS receptor 3 binds the B cell survival factor BAFF ligand through a discrete surface loop and promotes processing of NF-κB2. *Immunity* 17: 515–524.

36. Claudio, E., K. Brown, S. Park, H. Wang, and U. Siebenlist. 2002. BAFF-induced NEMO-independent processing of NF-κB2 in maturing B cells. *Nat. Immunol.* 3: 958–965.

37. Dejardin, E., N. M. Droin, M. Delhase, E. Haas, Y. Cao, C. Makris, Z. W. Li, M. Karin, C. F. Ware, and D. R. Green. 2002. The lymphotoxin-β receptor induces different patterns of gene expression via two NF-κB pathways. *Immunity* 17: 525–535.

38. Caamano, J. H., C. A. Rizzo, S. K. Durham, D. S. Barton, C. Raventos-Suarez, C. M. Snapper, and R. Bravo. 1998. Nuclear factor (NF)-κB2 (p100/p52) is required for normal splenic microarchitecture and B cell-mediated immune responses. *J. Exp. Med.* 187: 185–196.

39. Franzoso, G., L. Carlson, L. Poljak, E. W. Shores, S. Epstein, A. Leonardi, A. Grinberg, T. Tran, T. Scharton-Kersten, M. Anver, et al. 1998. Mice deficient in nuclear factor (NF)-κB/p52 present with defects in humoral responses, germinal center reactions, and splenic microarchitecture. *J. Exp. Med.* 187: 147–159.

40. Ishikawa, H., D. Carrasco, E. Claudio, R. P. Ryseck, and R. Bravo. 1997. Gastric hyperplasia and increased proliferative responses of lymphocytes in mice lacking the COOH-terminal ankyrin domain of NF-κB2. *J. Exp. Med.* 186: 999–1014.

41. Sivakumar, V., K. J. Hammond, N. Howells, K. Pfeffer, and F. Weih. 2003. Differential requirement for Rel/nuclear factor κB family members in natural killer T cell development. *J. Exp. Med.* 197: 1613–1621.

42. Elewaut, D., R. B. Shaikh, K. J. Hammond, H. De Winter, A. J. Leishman, S. Sidobre, O. Turovskaya, T. I. Prigozy, L. Ma, T. A. Banks, et al. 2003. NIK-dependent RelB activation defines a unique signaling pathway for the development of Vα 14i NKT cells. *J. Exp. Med.* 197: 1623–1633.

43. Akiyama, T., S. Maeda, S. Yamane, K. Ogino, M. Kasai, F. Kajiura, M. Matsumoto, and J. Inoue. 2005. Dependence of self-tolerance on TRAF6-directed development of thymic stroma. *Science* 308: 248–251.

44. Boehm, T., S. Scheu, K. Pfeffer, and C. C. Bleul. 2003. Thymic medullary epithelial cell differentiation, thymocyte emigration, and the control of autoimmunity require lympho-epithelial cross talk via LTβR. *J. Exp. Med.* 198: 757–769.

45. Galy, A. H., and H. Spits. 1992. CD40 is functionally expressed on human thymic epithelial cells. *J. Immunol.* 149: 775–782.

46. Dunn, R. J., C. J. Luedecker, H. S. Haugen, C. H. Clegg, and A. G. Farr. 1997. Thymic overexpression of CD40 ligand disrupts normal thymic epithelial organization. *J. Histochem. Cytochem.* 45: 129–141.

47. Gill, J., M. Malin, G. A. Hollander, and R. Boyd. 2002. Generation of a complete thymic microenvironment by MTS24⁺ thymic epithelial cells. *Nat. Immunol.* 3: 635–642.

48. Bennett, A. R., A. Farley, N. F. Blair, J. Gordon, L. Sharp, and C. C. Blackburn. 2002. Identification and characterization of thymic epithelial progenitor cells. *Immunity* 16: 803–814.

Alteration of intra-pancreatic target-organ specificity by abrogation of Aire in NOD mice

Shino Niki,[1] Kiyotaka Oshikawa,[1] Yasuhiro Mouri,[1] Fumiko Hirota,[1] Akemi Matsushima,[1] Masashi Yano,[1] Hongwei Han,[1] Yoshimi Bando,[2] Keisuke Izumi,[2] Masaki Matsumoto,[3,4] Keiichi I. Nakayama,[3,4] Noriyuki Kuroda,[1] and Mitsuru Matsumoto[1]

[1]Division of Molecular Immunology, Institute for Enzyme Research, University of Tokushima, Tokushima, Japan. [2]Department of Molecular and Environmental Pathology, Institute of Health Biosciences, University of Tokushima Graduate School, Tokushima, Japan. [3]Department of Molecular and Cellular Biology, Medical Institute of Bioregulation, Kyushu University, Fukuoka, Japan. [4]Core Research for Evolutional Science and Technology, Japan Science and Technology Corp., Saitama, Japan.

Factors that determine the spectrum of target organs involved in autoimmune destruction are poorly understood. Although loss of function of autoimmune regulator (AIRE) in thymic epithelial cells is responsible for autoimmunity, the pathogenic roles of AIRE in regulating target-organ specificity remain elusive. In order to gain insight into this issue, we have established NOD mice, an animal model of type 1 diabetes caused by autoimmune attack against β cell islets, in which Aire has been abrogated. Remarkably, acinar cells rather than β cell islets were the major targets of autoimmune destruction in Aire-deficient NOD mice, and this alteration of intra-pancreatic target-organ specificity was associated with production of autoantibody against pancreas-specific protein disulfide isomerase (PDIp), an antigen expressed predominantly by acinar cells. Consistent with this pathological change, the animals were resistant to the development of diabetes. The results suggest that Aire not only is critical for the control of self-tolerance but is also a strong modifier of target-organ specificity through regulation of T cell repertoire diversification. We also demonstrated that transcriptional expression of PDIp was retained in the Aire-deficient NOD thymus, further supporting the concept that Aire may regulate the survival of autoreactive T cells beyond transcriptional control of self-protein expression in the thymus.

Introduction

IDDM results from autoimmune destruction of insulin-producing pancreatic β cells (1, 2). The nature of immune dysregulation leading to β cell destruction remains poorly understood, but it is clearly influenced by multiple genetic, environmental, and immunological factors. The NOD mouse is a widely used animal model of IDDM, sharing major characteristics with the human disease (3, 4). Multiple genetic loci that control disease susceptibility have been mapped (5). Experimentally, defective central tolerance has been implicated in at least part of the pathogenic process in NOD mice, and this defective tolerance appears to be caused by an intrinsic defect in the apoptosis process in NOD thymocytes during negative selection (6–8). However, since establishment of self-tolerance primarily depends on physical contact between thymocytes and thymic stroma (9), it is also important to characterize stromal factors that might regulate the diabetic process in NOD mice.

Mutation of the autoimmune regulator (AIRE) gene is responsible for the development of an organ-specific autoimmune disease (autoimmune polyendocrinopathy–candidiasis–ectodermal dystrophy [APECED]) that demonstrates monogenic autosomal recessive inheritance (10, 11). As expected, deletion of the Aire gene in mice also results in the development of organ-specific autoimmune disease, although there are differences in target-organ specificity between human patients and Aire-deficient mice (12–14). Because medullary thymic epithelial cells (TECs) play pivotal roles in the cross-

talk between developing thymocytes and thymic stroma (15), and Aire-deficient TECs show reduced transcription of a group of genes encoding peripheral antigens (13, 14, 16), it is reasonable to speculate that pathogenic autoreactive T cells escape negative selection because of reduced expression of the corresponding target antigens in the Aire-deficient thymus (13, 17). However, other mechanisms of Aire-dependent tolerance also remain possible. Indeed, we have demonstrated that Aire-deficient mice develop autoimmunity against a transcriptionally unrepressed target antigen in the thymus (14). We therefore speculated that Aire might additionally regulate the processing and/or presentation of self-proteins so that maturing T cells can recognize self-antigens in a form capable of efficiently triggering autoreactive T cells. This alternative view of the function of Aire in the establishment of central tolerance has recently been supported by a study with transgenic mice expressing a model antigen under the control of a tissue-specific promoter together with a TCR specific for the corresponding antigen in the absence of Aire (18).

An important aspect of the study of autoimmune disease is target-organ specificity. Clearly, β cell islets are the predominant target of autoimmune attack in NOD mice, although the exact molecule(s) recognized by autoreactive T cells is still under debate (19). Similarly, autoimmune attack is mostly confined to the exocrine organs, such as salivary and lacrimal glands, in our Aire-deficient mice, except for the additional development of gastritis in mice on a BALB/c background (14). It remains largely unknown how target-organ specificity is defined by the NOD mouse background or by Aire deficiency in these animals.

In order to gain further insights into the contribution of AIRE to the establishment of central tolerance, as well as the pathogenic roles of AIRE in regulating target-organ specificity, we have established NOD mice lacking Aire. Aire-deficient NOD mice demonstrated both expected and unexpected autoimmune phenotypes. As

A

B

C
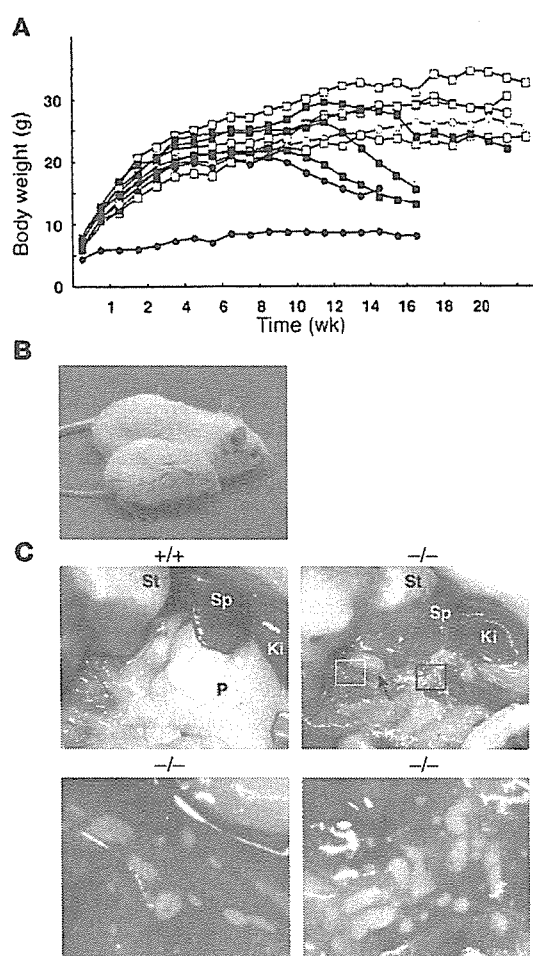
Figure 1
Growth abnormalities and pancreatic atrophy in Aire-deficient NOD mice. (**A**) Body weights of individual female (circles) and male (squares) Aire-sufficient (open symbols) and Aire-deficient (filled symbols) mice after birth were plotted. Measurement for many Aire-deficient NOD mice was terminated around 15–17 weeks after birth because of their lethal phenotypes. (**B**) Growth retardation of Aire-deficient NOD mice. Littermates of 7-week-old males are shown. (**C**) Pancreatic mass was absent from many Aire-deficient NOD mice upon gross inspection. Instead, many small white patches were scattered throughout the thin and lucent adipose tissues. The square areas marked with white and black lines are enlarged and shown in the bottom left and bottom right panels, respectively. An arrow (in the top right panel) indicates an enlarged pancreatic lymph node. Original magnification, ×1.2. Ki, kidney; P, pancreas; Sp, spleen; St, stomach.

strated the presence of some additional factor(s) that determines the target-organ specificity of the autoimmune disease caused by Aire deficiency; Aire-deficient BALB/c mice, but not Aire-deficient C57BL/6 mice, additionally show lymphoid cell infiltration in the gastric mucosa (14). In turn, we asked whether NOD mice lacking Aire might develop augmented autoimmune phenotypes and/or distinct target-organ specificity compared with NOD mice possessing Aire. We backcrossed our original strain of Aire-deficient mice to NOD mice for 6–9 generations. Heterozygous Aire-deficient mice were crossed to obtain homozygous Aire-deficient NOD offspring. Offspring homozygous for Aire deficiency were recognized in numbers slightly lower than expected from the heterozygous crossing when assessed 4 weeks after birth: $Aire^+/Aire^-/Aire^- = 64:111:44$ (mice backcrossed onto NOD for 7–9 generations were subjected to the analysis). Remarkably, many Aire-deficient NOD mice exhibited body-weight loss starting from 8–12 weeks after birth, as revealed by monitoring of 1 group of littermates chosen randomly (Figure 1A). More strikingly, one-third of Aire-deficient NOD mice (11 of 27 females and 8 of 30 males) demonstrated marked growth retardation from the neonatal stage (i.e., less than 50% of the body weight of their control littermates) with a gaunt appearance (Figure 1, A and B). Upon gross inspection of the organs, we noticed reduction of pancreas size (including the fat tissues surrounding the pancreas) in most of the Aire-deficient NOD mice, or even almost complete loss of pancreatic mass in one-third of the animals (Figure 1C, top right panel). In the latter animals, we observed many white patches 1–2 mm in size scattered throughout the thin and lucent adipose tissues (Figure 1C, bottom panels). These patches consisted of β cell islets, pancreatic ducts, and marked lymphoid cell infiltrations (see below). Pancreatic lymph nodes (Figure 1C, top right panel) together with other peripheral lymph nodes, such as submandibular and axillary lymph nodes (data not shown), were enlarged in many animals.

Upon histological evaluation, we observed marked lymphoid cell infiltration in various organs from Aire-deficient NOD mice, with 2 particular characteristics. First, the degree of lymphoid cell infiltration of the organs affected in the original (i.e., Aire-sufficient) NOD mice was much more severe in Aire-deficient NOD mice. Most pancreatic islets from many Aire-deficient NOD mice were surrounded by massive lymphoid cell infiltration, as if the β cell islets were floating on a sea of lymphoid cells (Figure 2A, bottom left panel). Furthermore, in many cases, the massive lymphoid cell infiltration completely destroyed acinar structures, leaving relatively well-preserved β cell islets together with pancreatic ducts densely surrounding the β cell islets alone (Figure 2A, middle panels). The degree of lymphoid cell infiltration in the salivary glands, which occurs in the original
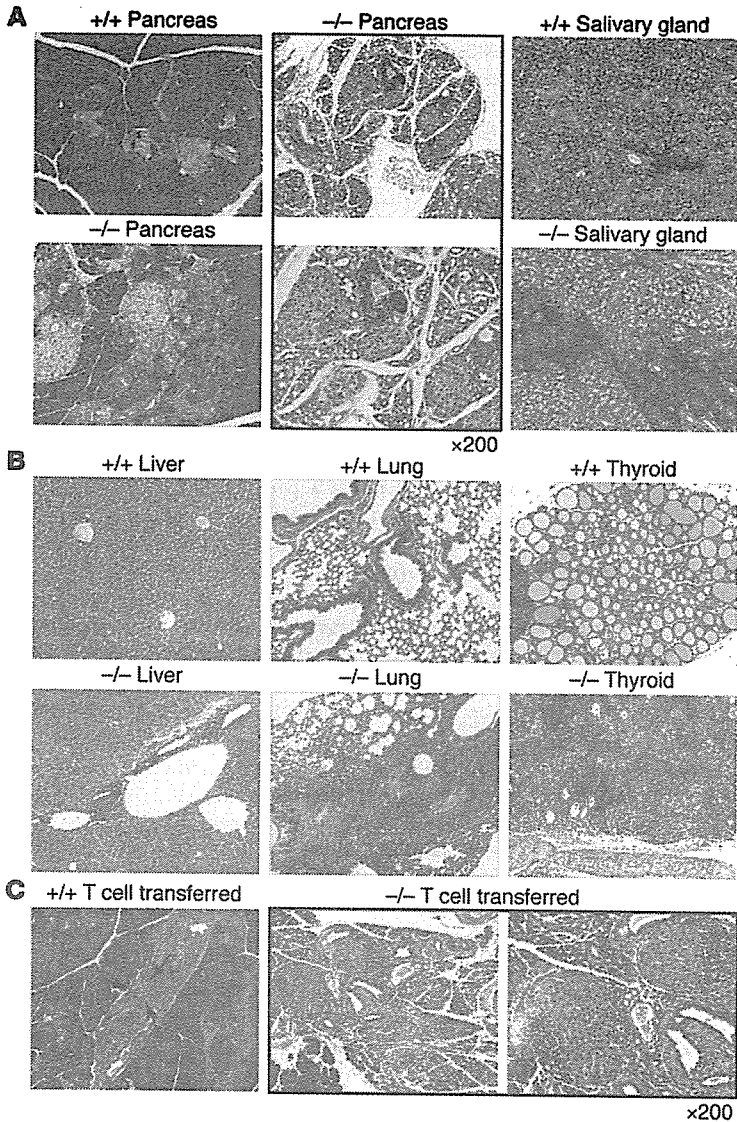
expected, we found obviously augmented autoimmune disease with early onset, which may be explained by the combined effect of the intrinsic NOD T cell defect together with the stromal abnormality resulting from lack of Aire, both of which affect central tolerance. Unexpectedly, we found resistance to the development of overt diabetes in Aire-deficient NOD mice, and this resulted from a change in the target cells attacked by the autoreactive T cells: acinar cells rather than β cell islets were the major targets of autoimmune destruction in Aire-deficient NOD mouse pancreas. Consistent with this alteration of intra-pancreatic target-organ specificity, we identified pancreas-specific protein disulfide isomerase (PDIp), a molecule expressed predominantly by acinar cells (20, 21), as an autoantigen recognized by Aire-deficient NOD mouse serum. Polyclonal B cell activation in Aire-deficient NOD mice was another unexpected feature in light of the fact that both Aire deficiency and NOD mice are considered to be models of organ-specific autoimmunity rather than systemic autoimmunity. Our studies with Aire-deficient mice on an autoimmune-prone NOD mouse background highlight novel aspects of Aire in the pathogenesis of autoimmune disease.

Results

Augmented autoimmune phenotypes in NOD mice lacking Aire. We have recently demonstrated that Aire-deficient mice develop Sjögren syndrome–like pathological changes in their exocrine organs (14). With the use of inbred Aire-deficient mouse strains, we have also demon-

A

+/+ Pancreas   –/– Pancreas   +/+ Salivary gland

–/– Pancreas   –/– Salivary gland

×200

B

+/+ Liver   +/+ Lung   +/+ Thyroid

–/– Liver   –/– Lung   –/– Thyroid

C   +/+ T cell transferred   –/– T cell transferred

×200

Figure 2

Augmented autoimmune phenotypes with altered intra-pancreatic target-organ specificity in Aire-deficient NOD mice. (**A**) Augmentation of existing autoimmune phenotypes of NOD mice by abrogation of Aire. In Aire-deficient NOD mice, lymphocytic infiltration in the pancreas was much more severe than that in control littermates (left panels). In many Aire-deficient NOD mice, acinar tissues were completely destroyed by marked lymphocytic infiltration, leaving relatively well-preserved β cell islets together with pancreatic ducts densely surrounding the β cell islets alone (middle panels). The 2 boxed panels are photographs taken of the same sample with different magnifications. Sialoadenitis was also much more severe in Aire-deficient NOD mice (right panels). (**B**) Lymphoid cell infiltration in the liver, lung, and thyroid gland from Aire-deficient NOD mice. (**C**) NOD-scid mice transferred with mature T cells purified from Aire-deficient NOD mice showed lymphocytic infiltration predominantly in acinar tissues, and the structure of the β cell islets was relatively well preserved (middle and right panels). In contrast, NOD-scid mice transferred with Aire-sufficient NOD mouse T cells showed lymphocytic infiltration into β cell islets, resulting in reduced size and numbers of β cell islets (left panel). Arrows indicate the 1 small β cell islet remaining. Original magnification, ×100, except where indicated.

NOD mice, was also much more severe in Aire-deficient NOD mice (Figure 2A, right panels). Secondly, we observed lymphoid cell infiltration in many other organs of Aire-deficient NOD mice, including liver, lung, and thyroid gland (Figure 2B) and prostate and seminal vesicle in males (Supplemental Table 1 and data not shown; supplemental material available online with this article; doi:10.1172/JCI26971DS1), in which we usually do not observe changes in the original NOD mice. Thus, abrogation of Aire in NOD mice resulted in expansion of the spectrum of target organs destroyed by autoimmune attack together with an alteration of intra-pancreatic target-organ specificity from β cell islets to acinar cells (see below). The growth abnormalities seen in Aire-deficient NOD mice described above might be partially explained by the digestive problems caused by loss of the exocrine pancreas, which has also been suggested in a recent study of Aire-deficient NOD mice (22).

Total spleen cell numbers were indistinguishable between Aire-deficient NOD mice and control littermates (i.e., Aire-sufficient NOD mice). Flow-cytometric analysis showed similar expression of B220, CD3, CD4, and CD8 in the spleen (data not shown). Small numbers of Aire-deficient NOD mice (i.e., 6 of 33 analyzed) showed

reduced numbers of total thymocytes together with reduction of CD4+CD8+ T cells to variable degrees. The pathological significance of this phenomenon is currently unclear. Despite the augmented autoimmune phenotypes in Aire-deficient NOD mice, the percentages of Foxp3+ Tregs from both thymus and spleen were not altered in the absence of Aire (Figure 3A), as we and others have reported for Aire-deficient mice on non–autoimmune-prone mouse backgrounds (14, 18). Expression of other T cell surface markers, such as CD25, CD62L, and CD69, on splenic T cells was also unchanged in Aire-deficient NOD mice (data not shown). In contrast, CD44^high (memory/activated) and ICOS-expressing populations of splenic CD4+ cells were increased in Aire-deficient NOD mice (Figure 3B).

Immunohistochemical analysis of the Aire-sufficient NOD thymus demonstrated indistinguishable numbers and distribution pattern of medullary TECs, as detected by *Ulex europaeus* agglutinin 1 (UEA-1) and ER-TR5 mAb (14, 23), with patterns of Aire nuclear dots similar to those from wild-type C57BL/6 and BALB/c thymus (Supplemental Figure 1, A and B, top panels); the subcellular distribution of Aire nuclear dots within the cell was also unaltered. Abrogation of Aire in NOD mice did not cause any abnormalities of TEC struc-

– 86 –
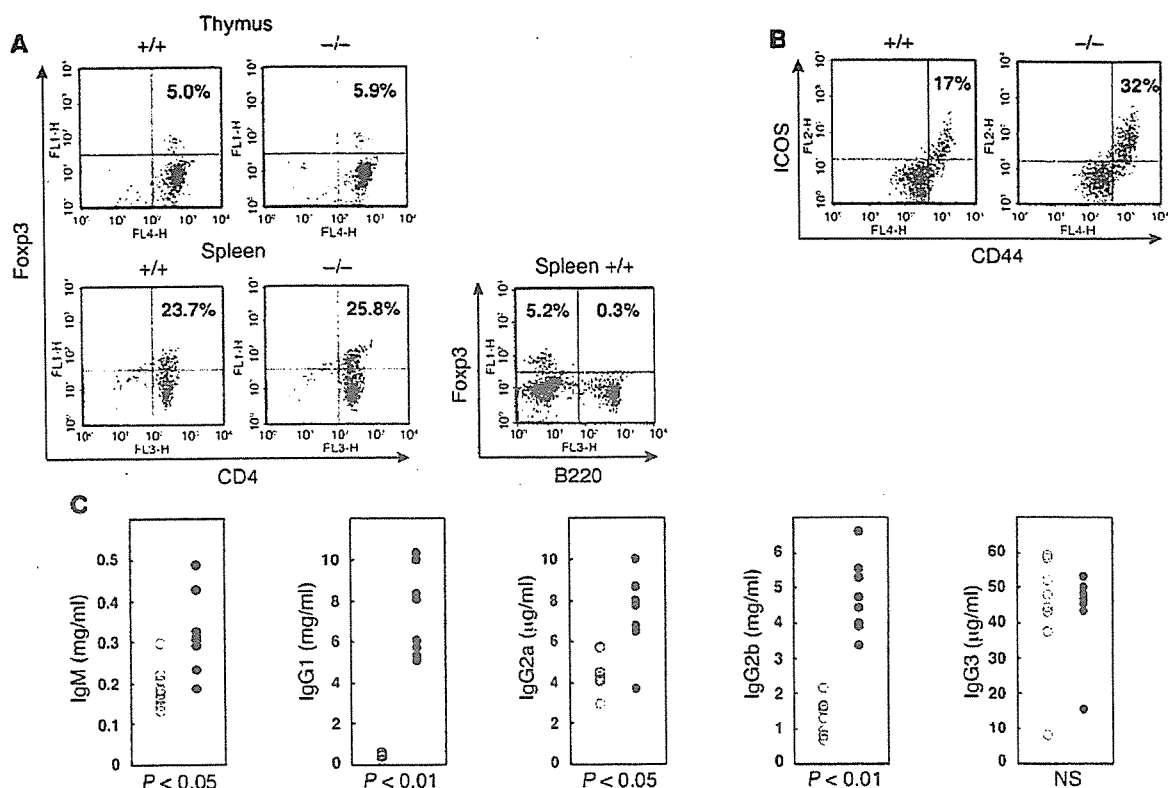
Figure 3
Phenotypic analyses of lymphocytes from Aire-deficient NOD mice. (A) Production of Tregs was retained in Aire-deficient NOD mice. CD3+ cells from the thymus and spleen were gated and analyzed for the expression of CD4 and Foxp3. Percentages of CD4+Foxp3+ cells are indicated. In order to verify the specificity of the staining, spleen cells from control mice were stained with anti-Foxp3 mAb. Foxp3+ cells were detected only in the B220− cell population, not in the B220+ cell population. (B) Memory/Activated (CD44high) ICOS+ cells were increased in the spleens from Aire-deficient NOD mice compared with the spleens from control mice. Percentages of CD44highICOS+ cells are indicated. CD4+ cells were gated and analyzed for CD44 and ICOS expression. (C) Serum Ig levels were elevated in Aire-deficient NOD mice (filled circles) compared with Aire-sufficient NOD littermates (open circles) except for IgG3. One mark corresponds to 1 mouse analyzed.

ture recognized by UEA-1 and ER-TR5 (Supplemental Figure 1A, bottom panels). Expression of several, but not all, of the tissue-specific genes tested, including *insulin*, in the TECs isolated from Aire-deficient NOD mice was reduced, as previously observed in Aire-deficient mice of non-autoimmune-prone mouse backgrounds (Table 1) (13, 14, 16). RNAs extracted from the total thymus of Aire-deficient NOD mice showed similar reduced expression of tissue-specific genes, including *insulin* (Supplemental Table 2).

Alteration of intra-pancreatic target-organ specificity in Aire-deficient NOD mice. Aire-deficient NOD mice started to exhibit lymphoid cell infiltration into the pancreas between 2 and 3 weeks after birth; although these changes were not observed at 1 week after birth (0 of 1 female examined), Aire-deficient NOD mice at 2 weeks (1 male of 1 female and 1 male) and 3 weeks (2 of 2 males) showed peri-insular lymphocytic infiltration (data not shown). In contrast, none of their control littermates showed those changes in the pancreas at less than 3 weeks (0 of 2 females and 2 males). This result suggests that abrogation of Aire in NOD mice not only augments the degree of pancreatic lesions once developed, as described above, but also accelerates their onset. Similarly, development of sialoadenitis was accelerated in Aire-deficient NOD mice (S. Niki and M. Matsumoto, unpublished data).

The pancreas is unique in that it functions as both an endocrine and an exocrine organ by secreting insulin as well as several digestive

enzymes such as trypsinogen, amylase, and lipase. Careful histological evaluation of the pancreatic lesions in Aire-deficient NOD mice showed unique features of the pathological changes, as described above. The initial change in the pancreas from Aire-deficient NOD mice was perivascular lymphoid cell infiltration near the β cell islets, as observed in control littermates (Y. Bando et al., unpublished data). In control mice, lymphoid cell infiltration was directed into β cell islets, eventually destroying them and leading to the complete loss of insulin-producing cells (data not shown). In marked contrast, in Aire-deficient NOD mice, although lymphoid cell infiltration became more evident as the mice grew, the histological picture of β cell islets being progressively invaded by lymphoid cells was barely apparent (Figure 2A). Instead, acinar tissues surrounding the β cell islets were replaced by infiltrating CD4+, CD8+, and B220+ cells (Supplemental Figure 2). In addition to B220+ cells (Supplemental Figure 2B, top panels), clusters of CD138+ (syndecan-1+) cells expressing low levels of B220 were also observed (Supplemental Figure 2B, bottom panels). The outcome of this unusual immune attack in Aire-deficient NOD mice was the complete disappearance of acinar structures, leaving behind relatively well-preserved β cell islets and pancreatic ducts densely surrounding the β cell islets, which, together with infiltrating lymphoid cells, formed visible white patches throughout the adipose tissues, as demonstrated

Table 1

Expression of tissue-specific genes from TECs in Aire-deficient NOD mice

Genotype	Foxn1/Hprt	Ins/Hprt	SP1/Hprt	FABP/Hprt	CRP/Hprt	GAD67/Hprt	PDIp/Hrpt
+/+	8.10	2.54×10^{-1}	6.52	6.98	4.55	30.8	1.91
–/–	10.0	UD	UD	9.27×10^{-2}	8.63	53.2	1.59
Relative abundance (Aire KO/control)	1.23	ND	ND	1/75.3	1.90	1.73	0.83

Real-time PCR for *Foxn1* and peripheral tissue-specific genes (*Ins*, insulin; *SP1*, salivary protein 1; *FABP*, fatty acid–binding protein; *CRP*, C-reactive protein; *GAD67*, glutamic acid decarboxylase 67; *PDIp*) was performed using thymic-stroma RNAs from control and Aire-deficient NOD mice. *Hprt* expression level was used as an internal control. The relative abundance of each gene was calculated from the ratio between the values from control NOD thymus and those from Aire-deficient NOD thymus (e.g., the *insulin/Hprt* value from Aire-deficient NOD mice was divided by the *insulin/Hprt* value from control NOD mice). Pools of TECs isolated from 2 mice of each group were used for the analysis. Mice backcrossed onto NOD mice for 6 generations were used. UD, under the limit of detection; ND, not determined.

above (Figures 1C and 2A). Thus, abrogation of Aire in NOD mice resulted in the dramatic alteration of intra-pancreatic target-organ specificity from endocrine cells toward exocrine cells.

Resistance to diabetes development in Aire-deficient NOD mice. Aire-deficient NOD mice rarely survived more than 20 weeks (Figure 1A), probably because of the severe autoimmune phenotype. By the ages of 12 and 22 weeks, respectively, 1 Aire⁺⁻ female and 1 Aire⁺⁻ female had developed overt diabetes, out of 48 control mice (10 Aire⁻⁺ females, 12 Aire⁻ males, 17 Aire⁻ females, and 9 Aire⁺⁻ males) monitored for the development of diabetes. In contrast, none of the Aire-deficient NOD mice (11 females and 12 males) developed overt diabetes during the same series of observations, which was a predictable consequence of the fact that Aire-deficient NOD mice demonstrated immune attack predominantly against acinar cells rather than β cell islets. Absence of hyperglycemia in Aire-deficient NOD mice was not simply caused by feeding problems, since the stomachs of all the Aire-deficient NOD mice were found to be full of food when the animals were sacrificed (S. Niki and M. Matsumoto, unpublished data).

In order to evaluate whether Aire-deficient NOD mice are intrinsically resistant to the development of diabetes, we used an induced-diabetes model. We treated mice with cyclophosphamide (CY), an immunosuppressive drug that accelerates diabetic processes in diabetes-prone mice (24, 25). Thirteen of 18 control littermates in a total of 3 experiments developed overt diabetes between 11 and 27 days (mean 19.2 days) after the initial injection of CY (Table 2). Although 9 of 11 Aire-deficient NOD mice were unable to tolerate CY treatment and died or were sacrificed between 7 and 22 days (mean 16.8 days) after the initial injection of CY, and only 2 Aire-deficient NOD mice survived throughout this observation period, none of them showed overt diabetes. This result supports the concept that abrogation of Aire in NOD mice results in resistance to development of diabetes, most probably because of alteration of intra-pancreatic target-organ specificity, and this hypothesis was further confirmed by another experiment (see below). A glucose tolerance test performed by i.p. injection of glucose (2 mg/g body weight) into 4 Aire-deficient NOD mice (a 10-week-old male, a 14-week-old female, a 16-week-old male, and a 20-week-old male) also revealed no diabetic pattern in these animals (S. Niki and M. Matsumoto, unpublished data).

Alteration of intra-pancreatic target-organ specificity accounts for the resistance to development of diabetes in Aire-deficient NOD mice. In order to confirm that Aire-deficient NOD mice are resistant to the development of diabetes as a result of alteration of intra-pancreatic target-organ specificity, we evaluated the disease process by transferring mature T cells isolated from either control littermates or Aire-deficient NOD mice into NOD-scid mice (26). In a first set of experi-

ments, 3 of 5 NOD-scid mice transferred with control mouse T cells developed diabetes at 77, 120, and 140 days after the transfer (Table 3, experiment 1); 1 NOD-scid mouse transferred with Aire-sufficient

Table 2

CY-induced diabetes

	Genotype	Sex	Diabetes development (onset from first dose)
Exp. 1ᴬ	+/+	M	Yes (day 27)
	+/+	M	No
	+/–	M	Yes (day 11)
	–/–	M	No
	–/–	M	No
	–/–	M	ND (sacrificed on day 11)
Exp. 2ᴮ	+/+	M	Yes (day 13)
	+/+	M	No
	+/–	F	Yes (day 13)
	+/–	F	Yes (day 25)
	+/–	M	Yes (day 20)
	–/–	F	ND (died on day 20)
	–/–	F	ND (died on day 20)
	–/–	M	ND (sacrificed on day 20)
Exp. 3ᶜ	+/+	F	Yes (day 11)
	+/+	F	Yes (day 22)
	+/+	M	Yes (day 27)
	+/+	M	No
	+/+	M	No
	+/–	F	Yes (day 14)
	+/–	F	Yes (day 22)
	+/–	F	Yes (day 22)
	+/–	F	Yes (day 22)
	+/–	M	No
	–/–	F	ND (died on day 7)
	–/–	F	ND (died on day 22)
	–/–	F	ND (died on day 22)
	–/–	M	ND (died on day 7)
	–/–	M	ND (died on day 22)

CY dissolved in PBS was injected i.p. (0.2 mg/g body weight) into mice on day 0 and day 14. Blood glucose levels were measured every day, and mice were diagnosed as diabetic when blood glucose levels exceeded 250 mg/dl. Observation was terminated 28 days after the first CY injection. ᴬNine-week-old mice backcrossed onto NOD mice for 6 generations were used for the experiment. ᴮSeven-week-old mice backcrossed onto NOD mice for 6 generations were used for the experiment. ᶜNine-week-old mice backcrossed onto NOD mice for 8 and 9 generations were used for the experiment. Exp., experiment; ND, not determined (reason described in parentheses).

Table 3
Development of diabetes in NOD-scid mice transferred with mature T cells

Donor		Diabetes development	BW (g)	Histology of pancreas		
				Peri-insular lymphocytic infiltration	Loss of β cell islets	Atrophy of acinar tissues
Exp. 1[A]	+/+	ND (sacrificed on day 51)	19.3	++	−	−
	+/+	Yes (day 77)	22.1	++	+	−
	+/+	Yes (day 120)	24.6	++	++	−
	+/+	Yes (day 140)	23.3	+	++	−
	+/+	No	24.4	++	−	−
	−/−	ND (sacrificed on day 51)	12.4	++	+	+
	−/−	ND (died on day 57)	ND (not available)	ND (not available)	ND (not available)	ND (not available)
	−/−	No	18.4	++	−	++
	−/−	No	17.2	++	−	++
	−/−	No	17.6	++	−	++
Exp. 2[B]	+/+	Yes (day 77)	21.6	+	++	−
	+/+	ND (sacrificed on day 95)	20.8	++	++	−
	−/−	ND (sacrificed on day 90)	15.4	++	−	+
	−/−	ND (sacrificed on day 95)	17.2	++	−	+
	−/−	ND (sacrificed on day 95)	16.2	++	+	+

Thy1^{+} cells purified from 7-week-old female mouse spleens of either 3 control mice or 3 Aire-deficient NOD mice were injected i.v. into 8-week-old female NOD-scid mice (4 × 10^6 cells per mouse). and development of diabetes was monitored for 20 weeks. Blood glucose levels were measured every week. and mice were diagnosed as diabetic when blood glucose levels exceeded 250 mg/dl. [A]Mice backcrossed onto NOD mice for 6 generations were used. [B]Mice backcrossed onto NOD mice for 8 generations were used. BW. body weight. ++. severe: +. moderate: −. not remarkable.
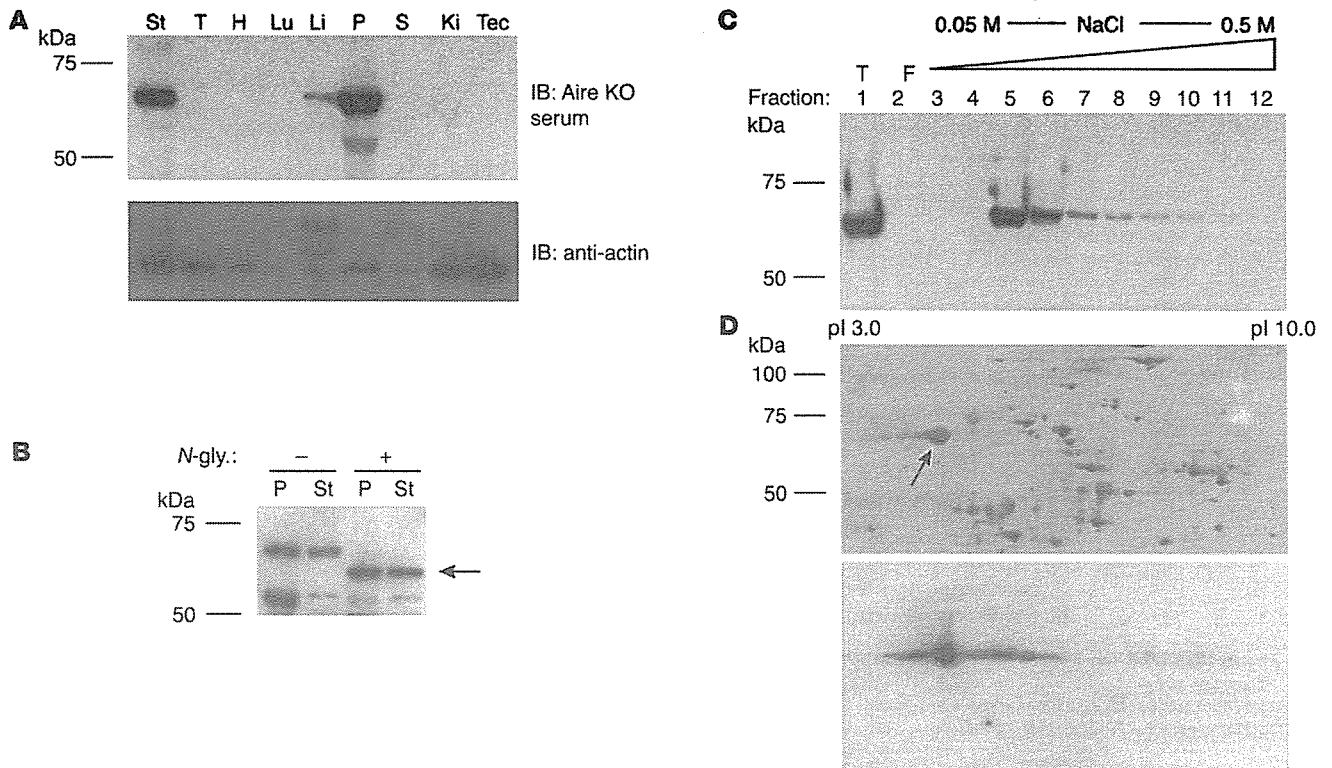
NOD mouse T cells was sacrificed at day 51 for histological comparison with a NOD-scid mouse transferred with Aire-deficient NOD mouse T cells. In contrast, none of the NOD-scid mice transferred with Aire-deficient NOD mouse T cells developed diabetes; we had to sacrifice 1 mouse at day 51 because of severe sickness, and another mouse died during the observation period (Table 3, experiment 1). All the mice transferred with Aire-deficient NOD mouse T cells showed body-weight loss before sacrifice. It is important to mention that we used splenic T cells isolated from Aire-deficient NOD mice before their body-weight loss had begun (i.e., 7 weeks old). Furthermore, flow-cytometric analysis of thymocytes and splenocytes isolated from the Aire-deficient NOD mouse donors used in this experiment showed no obvious changes compared with those from control mice (data not shown).

Histological evaluation showed that the NOD-scid mice transferred with Aire-deficient NOD mouse T cells recapitulated the pathological changes seen in untreated Aire-deficient NOD mice; acinar tissues were severely destroyed by the infiltrating lymphoid cells, and only pancreatic ducts and relatively well-preserved β cell islets remained (Figure 2C and Table 3). In contrast, reduced size and numbers of β cell islets with lymphoid cell infiltration were the predominant pathological features of NOD-scid mice transferred with control mouse T cells, as seen in untreated Aire-sufficient NOD mice (Figure 2, A and C). These results indicate that Aire-deficient NOD mice are resistant to the development of diabetes as a result of alteration of intra-pancreatic target-organ specificity from β cell islets toward acinar cells. A second set of experiments with more backcrossed mice showed similar results (Table 3, experiment 2).

Polyclonal B cell activation in Aire-deficient NOD mice. Serum IgM and all subclasses of IgG except for IgG3 were significantly elevated in Aire-deficient NOD mice (Figure 3C). These increased serum Ig levels, together with augmented autoimmunity in Aire-deficient NOD mice, as described above, were associated with the produc-

tion of autoantibodies against various organs. When serum from Aire-deficient NOD mice was tested for reactivity against pancreas, stomach, kidney, and liver, all sera contained autoantibodies of the IgG class against the broad spectrum of organs, as detected with immunofluorescence (Supplemental Figure 3 and Supplemental Table 3). Interestingly, autoantibodies from Aire-deficient NOD mice reacted with acinar cells more strongly than with β cell islets in the pancreas (Supplemental Figure 3, top right panel), which is consistent with the predominant autoimmune attack against acinar cells. In contrast, no such activities were observed in sera from control littermates. These results suggest induction of polyclonal B cell activation in Aire-deficient NOD mice, which has not been observed either in Aire-deficient mice with non-NOD backgrounds (13, 14) or in the original NOD mice. This was unexpected, because both Aire-deficient mice and NOD mice are considered to be models of T cell–mediated organ-specific autoimmunity rather than systemic autoimmunity. Serum cytokine levels, including those of IFN-α, IL-2, IL-4, and IL-6, in Aire-deficient NOD mice were below the limit of detection, as with control littermates. Expression of B cell surface markers, such as CD40, CD80, CD86, and B7-related protein 1 (B7RP-1), on splenic B cells was also unchanged in Aire-deficient NOD mice (S. Niki et al., unpublished data).

Identification of PDIp as an autoantigen recognized by Aire-deficient NOD mouse serum. Preferential recognition of acinar cells by Aire-deficient NOD mouse serum with immunofluorescence prompted us to identify target antigen(s) that might be associated with an alteration of intra-pancreatic target-organ specificity. We first characterized target antigen(s) by Western blot analysis using proteins extracted from the pancreas as well as other tissues (Figure 4A). Protein extracted from the pancreas showed a discrete band of approximately 65 kDa, and this was observed in all the Aire-deficient NOD mouse sera tested (10 of 10). A band of the same size was also observed from the protein extracted from the stomach. After N-glycosidase F treatment,

A

kDa   St   T   H   Lu   Li   P   S   Ki   Tec

75 —

50 —

IB: Aire KO serum

IB: anti-actin

B

N-gly.:   —   +

kDa   P   St   P   St

75 —

50 —

C   0.05 M ——— NaCl ——— 0.5 M

     T   F

Fraction: 1   2   3   4   5   6   7   8   9   10   11   12

kDa

75 —

50 —

D

kDa   pI 3.0   pI 10.0

100 —

75 —

50 —

Figure 4

Identification of PDIp as an autoantigen recognized by Aire-deficient NOD mouse serum. (**A**) Detection of autoantigen from the stomach and pancreas with Western blot analysis using Aire-deficient NOD mouse serum. The same blot was probed with anti-actin Ab (bottom panel). St, stomach; T, thymus; H, heart; Lu, lung; Li, liver; P, pancreas; S, spleen; Ki, kidney; Tec, mouse thymic epithelial cell line. (**B**) The target antigen is present as a glycoprotein in both the pancreas and the stomach. After N-glycosidase F treatment (marked as "+"), both bands similarly migrated to lower positions (indicated by an arrow). Western blot analysis with Aire-deficient NOD mouse serum was used for the detection. P, pancreas; St, stomach. (**C**) Purification of autoantigen by anion-exchange chromatography. Each fraction eluted with increasing concentrations of NaCl was tested for the presence of autoantigen by Western blot analysis. T, total cell lysate; F, flow-through fraction. (**D**) Identification of autoantigen by 2-dimensional gel electrophoresis. Proteins from fraction 5 shown in **C** were subjected to 2-dimensional gel electrophoresis (top panel). Western blot analysis identified a discrete signal (bottom panel), and the corresponding spot in the gel was subjected to mass spectrometry (indicated by an arrow in the top panel). pI, isoelectric point.

both bands similarly migrated to lower positions, suggesting that the target antigen is a glycoprotein present in both the pancreas and the stomach (Figure 4B). Because epithelial cells from the stomach were easier to obtain and handle, we attempted to isolate the target antigen from these cells. After purification by anion-exchange chromatography, the target antigen was found to be present most abundantly in the fraction eluted with 0.15 M NaCl (Figure 4C, fraction 5), and therefore this fraction was further subjected to 2-dimensional gel electrophoresis (Figure 4D, top panel). Western blot analysis of the 2-dimensional gel revealed a discrete spot (Figure 4D, bottom panel), which was identified as PDIp by mass spectrometry. The change in the molecular weight of the target antigen after N-glycosidase F treatment (Figure 4B) was consistent with the characteristics of PDIp (20, 21). Furthermore, Aire-deficient NOD mouse serum, but not control mouse serum, showed reactivity against bacterially expressed glutathione-S-transferase–PDIp fusion protein, but not against glutathione-S-transferase alone (Supplemental Figure 4). Although PDIp was originally reported to be pancreas-specific in humans, we detected PDIp expression in the mouse stomach by Northern blot analysis (data not shown) and in fact identified PDIp as an autoantigen using proteins extracted from the stomach, as

described above. More importantly, it has been reported that PDIp is restricted to acinar cells in the pancreas, at least in humans (20, 21). Despite the development of autoimmunity against PDIp, transcriptional expression of *PDIp* was retained in TECs (Table 1) or total thymus (Supplemental Table 2) of Aire-deficient NOD mice.

Discussion

In order to gain further insight into the roles of AIRE in the establishment of central tolerance, we have established NOD mice lacking Aire. We specifically chose NOD mice because of their well-established intrinsic defect in thymocyte apoptosis during negative selection (6–8), hoping that the role of Aire as a stromal factor in central tolerance might be better investigated by combination with a defective reciprocal factor (i.e., pathogenic NOD thymocytes). The results highlighted unique features of Aire that control target-organ specificity. Although there are many examples of gene-targeted mice in which distinct target organs are involved in autoimmune destruction depending on the genetic background of the animal, as we have also reported for Aire-deficient mice (14), the results presented in this study are striking in that deletion of a single gene, *Aire*, altered a discrete target-organ specificity of NOD mice on a fixed genetic background.

Aire in TECs has been suggested to regulate promiscuous gene expression, thereby controlling autoimmunity (13). In fact, TECs isolated from Aire-deficient NOD mice showed reduced expression of several tissue-specific genes, including *insulin*, as observed in non–autoimmune-prone mouse backgrounds (13, 14, 16). Given that insulin is a prime target antigen recognized by autoreactive T cells in NOD mice (19), the finding that β cell islets were relatively less affected by autoimmune attack in Aire-deficient NOD mice, despite repressed *insulin* expression in their TECs (Table 1), does not support the concept that Aire-dependent transcriptional control of tissue-specific antigen genes in TECs accounts for Aire-dependent autoimmunity. Furthermore, thymic expression of *PDIp*, a tissue-specific antigen recognized by Aire-deficient NOD mouse serum, was not downregulated, as demonstrated in this study (Table 1 and Supplemental Table 2). Thus, there is still a lack of experimental evidence to connect the postulated roles of Aire in the transcriptional regulation of tissue-specific antigen expression with efficient elimination of autoreactive T cells. We currently favor the idea that Aire may regulate the processing and/or presentation of self-proteins in order for autoreactive T cells to be appropriately eliminated within the thymus (14, 18). In this regard, it is also noteworthy that bone marrow–derived cells, most likely DCs, in the thymus can acquire self-antigens presented by medullary TECs and cross-present them to developing thymocytes to enforce self-tolerance (27). It is therefore possible that loss of AIRE function in medullary TECs may result in insufficient uptake of self-proteins from medullary TECs by DCs necessary for cross-presentation.

Given that Tregs arise from relatively high-avidity interactions with self-peptide–MHC complexes just below the threshold for negative selection (28–30), it was somewhat unexpected that Aire deficiency had no major impact on the production as well as the suppressive function of Tregs in non–autoimmune-prone mouse backgrounds (14, 18). Similarly, we have demonstrated that the numbers of Foxp3⁺ Tregs were not changed in Aire-deficient mice even on an autoimmune-prone NOD mouse background (Figure 3A). This lack of a major impact of Aire on the production and/or function of Tregs appears to be supported by a recent report describing the phenotypes of NOD mice in which Tregs were depleted by in vivo IL-2 neutralization (31); the effect of in vivo IL-2 neutralization has mainly been attributed to the loss of homeostatic maintenance of Tregs. In contrast to the Aire-deficient NOD mice described in the present study, NOD mice depleted of Tregs showed early onset of diabetes (31). Furthermore, NOD mice depleted of Tregs demonstrated target-organ specificity, such as neuritis, different from that seen in Aire-deficient NOD mice. Thus, although it remains possible that in vivo IL-2 neutralization does more than deplete Tregs, the phenotypes of Aire-deficient NOD mice are different from those seen in NOD mice deficient in Tregs, suggesting that Aire does not play major roles in the regulation of Treg-mediated autoimmunity.

Numerous factors have been reported to modulate the diabetic process in NOD mice, many of which affect T cell function and/or communication between APCs and T cells, both mainly in the periphery (3, 32). Among these, one recent report merits attention (33). NOD mice deficient in programmed cell death 1 (PD-1), an immunoinhibitory receptor belonging to the CD28/CTL-associated antigen-4 family, exhibited accelerated and augmented insulitis compared with PD-1-sufficient NOD mice. Sialoadenitis was also accelerated in PD-1-deficient NOD mice. Of importance, other organs have never been reported to be affected by the absence of PD-1 despite the severe lesions of pancreas and salivary glands, suggest-

ing that target-organ specificity was maintained in NOD mice deficient in PD-1. In contrast, alteration of intra-pancreatic target-organ specificity together with an expansion of target-organ spectrum was observed in Aire-deficient NOD mice. The different effects of abrogation of PD-1 or Aire underscore the existence of autoimmune modulators with unique actions. PD-1 may be a general regulator of the autoimmune process without governing target-organ specificity, at least on the NOD background (33), whereas Aire additionally controls target-organ specificity on the same background.

We have identified PDIp as an autoantigen recognized by serum from Aire-deficient NOD mice. The pathogenic roles of anti-PDIp autoantibody in the alteration of intra-pancreatic target-organ specificity remain to be studied. Because NOD-scid mice inoculated with Aire-deficient NOD mouse T cells alone developed pancreatic lesions quite similar to those of untreated Aire-deficient NOD mice, production of anti-PDIp autoantibody may not be relevant to the disease process but could be secondary to the massive destruction of acinar cells. Nevertheless, as Aire-deficient NOD mice developed autoimmunity against PDIp, and PDIp expression is restricted to acinar cells (20, 21), Aire clearly plays a significant role in the alteration of intra-pancreatic target-organ specificity demonstrated in this study. Furthermore, identification of this tissue-specific antigen as an autoantigen recognized by Aire-deficient NOD mice helped us to strengthen our current model of Aire function described above, because α-fodrin, which we initially identified as an autoantigen that was not downregulated in Aire-deficient thymus, is a ubiquitous, but not tissue-specific, antigen (14).

It remains unexplained why the abrogation of Aire resulted in the alteration of intra-pancreatic target-organ specificity from β cell islets to acinar cells. Even though abrogation of Aire could additionally impair the presentation of pancreatic acinar-cell antigen(s), thereby provoking autoimmunity against these cells by a mechanism such as proposed above, autoreactivity against β cell islets (or possibly insulin) should still remain, and we would expect to see the development of diabetes in Aire-deficient NOD mice with at least a similar frequency to that in Aire-sufficient NOD mice. However, Aire-deficient NOD mice demonstrated resistance to the development of diabetes, both in their natural history and in 2 models of induced diabetes (CY injection and T cell transfer into NOD-scid mice). One possible explanation for this alteration of intra-pancreatic target-organ specificity is that establishment of self-tolerance for β-cell-islet antigen(s) and establishment of self-tolerance for acinar-cell antigen(s) are not independent processes in the negative selection niche in the thymus; impaired negative selection against acinar-cell antigen(s) by loss of Aire could, by an unknown mechanism, have relieved abnormal negative selection against β cell antigen(s). Alternatively, the capacity for autoimmune attack against β cell islets might have been exhausted by mobilization of immune cells toward the destruction of a better target in the form of neighboring acinar cells. The reasoning behind both these explanations may be much too simplistic, and better understanding of the nature of target-organ specificity as well as of the primary function of AIRE requires new experimental systems to approach these issues.

The finding that abrogation of Aire in NOD mice, even though it was achieved by a mechanism involving alteration of intra-pancreatic target-organ specificity, did not accelerate the development of diabetes is obviously inconsistent with the extremely early onset of diabetes in Aire-deficient double-transgenic mice with model antigens expressed in the thymus together with TCRs recognizing the corresponding antigens (18, 34). However, this discrepancy between

— 91 —

the present study and the transgenic studies does not argue against an essential role of Aire in the prevention of autoimmune disease. Rather, we think that the difference is simply due to the uniqueness of each model, in which Aire might exert different roles in the disease process. The function of Aire in controlling target-organ specificity was recognizable only in the present study, in which clonal diversification of thymocytes was possible during the course of negative selection. In contrast, prevention of an autoimmune process of fixed target-organ specificity (i.e., progression from innocuous insulitis to overt diabetes) was the predominant feature of Aire observed in the transgenic studies because of the predefined TCR specificities in which clonal diversification was not available (18, 34).

Because both Aire-deficient and NOD mice demonstrate organ-specific autoimmune pathology rather than a systemic autoimmunity such as SLE, the polyclonal B cell activation in Aire-deficient NOD mice was unexpected. Local Ig production by the CD138⁺ cell clusters in the pancreas might be responsible for the elevation of serum Ig levels (Supplemental Figure 2B). In this respect, it is possible to speculate that an Aire-deficient thymic microenvironment will produce more T cells of a certain subset(s) that promotes B cell maturation into plasma cells, in a manner similar to that in which follicular Th cells help to produce high titers of autoantibodies consistent with polyclonal B cell activation (35). In fact, flow-cytometric analyses of splenic T cells from Aire-deficient NOD mice have demonstrated increased percentages of the CD44^{high}ICOS⁺ population (Figure 3B). Interestingly, a gene-chip analysis of genes whose expression levels differed between Aire-deficient and control medullary TECs identified several genes that might affect T cell function and/or differentiation into distinct T cell subtypes, including genes involved in antigen processing and/or presentation and genes coding for chemokines (18).

Finally, a single report has suggested altered functions of Aire and/or Aire⁺ cells that could be relevant to the autoimmune phenotypes seen in NOD mice (36). Although NOD thymi have been shown by Western blot analysis to express Aire protein at normal levels, and the size and shape of the Aire nuclear dots from NOD thymus resembled the pattern seen in control thymus, as we have also observed (Supplemental Figure 1B), it was reported that Aire⁺ cells from NOD mice contained large intranuclear vacuoles that seemed to displace the Aire protein to the periphery of the nuclei, suggesting that abnormal functions of Aire and/or Aire⁺ cells in TECs may contribute to the development of the autoimmune phenotypes of NOD mice (36). Our present study, however, clearly demonstrated that abrogation of Aire in NOD mice modulated the autoimmune phenotypes of NOD mice, suggesting that Aire and/or Aire⁺ cells in NOD mice are functionally competent.

In conclusion, our present study has provided unique insights into the roles of Aire in the pathogenesis of organ-specific autoimmune disease through combination with the autoimmune-prone NOD mouse model. In turn, we have obtained novel perspectives on the autoimmune process in NOD mice through loss of the fundamental stromal function of Aire. More generally, we believe that understanding the relationship between *AIRE* gene malfunction and the breakdown of self-tolerance promises to help unravel the pathogenesis not only of APECED but also of other types of autoimmune disease.

Methods

Mice. NOD/Shi Jic mice and NOD/Shi-scid Jic mice were purchased from CLEA Japan Inc., and Rag2-deficient mice on a BALB/c background were from Taconic. Aire-deficient mice of mixed background (H-2^{b/k} × H-2^b)

were generated as previously reported (14). The mice were maintained under pathogen-free conditions and were handled in accordance with the Guidelines for Animal Experimentation of University of Tokushima School of Medicine. All animal experiments were approved by the Animal Experimentation Committee of Tokushima University.

Pathology. Formalin-fixed tissue sections were subjected to H&E staining, and 2 pathologists independently evaluated the histology without being informed of the detailed condition of the individual mouse.

Flow-cytometric analysis. Thymus and spleen cell suspensions were stained with the following mAbs: anti-CD45R/B220, anti-CD3, anti-CD4, anti-CD8, anti-CD44, and anti-Foxp3 (eBioscience). Staining for Foxp3-expressing cells was performed according to the manufacturer's instructions.

Immunohistochemistry. Immunohistochemical analysis of the thymus with ER-TR5 (37) and UEA-1-FITC (Vector Laboratories) was performed as previously described (23). Polyclonal anti-Aire Ab was produced by immunization of rabbits with peptides corresponding to the COOH-terminal portion of mouse Aire, and Alexa 488–conjugated donkey anti-rabbit IgG (Invitrogen Corp.) was used as a secondary Ab for detection. For the detection of autoantibodies, mouse serum was incubated with various organs obtained from Rag2-deficient mice. FITC-conjugated anti-mouse IgG Ab (Southern Biotechnology Associates Inc.) was used for detection (23).

TEC preparation. TECs were prepared as described previously (14). Briefly, thymic lobes were isolated from 2 mice for each group and cut into small pieces. The fragments were gently rotated in RPMI 1640 medium (Invitrogen Corp.) supplemented with 10% heat-inactivated FCS (Invitrogen Corp.), 20 mM HEPES, 100 U/ml penicillin, 100 μg/ml streptomycin, and 50 μM 2-mercaptoethanol at 4°C for 30 minutes, and dispersed further with pipetting to remove the majority of thymocytes. The resulting thymic fragments were digested with 0.125% collagenase D (Roche Molecular Biochemicals) and 10 U/ml DNase I (Roche Molecular Biochemicals) in RPMI 1640 at 37°C for 15 minutes. The supernatants, containing dissociated TECs, were saved, and the remaining thymic fragments were further digested with collagenase D and DNase I. This step was repeated twice, and the remaining thymic fragments were digested with 0.125% collagenase/dispase (Roche Applied Science) and DNase I at 37°C for 30 minutes. The supernatants from this digest were combined with the supernatants from the collagenase digests, and the mixture was centrifuged for 5 minutes at 450 g. The cells were suspended in PBS containing 5 mM EDTA and 0.5% FCS and kept on ice for 10 minutes. CD45⁻ thymic stromal cells were then purified by depletion of CD45⁺ cells with MACS CD45 MicroBeads (Miltenyi Biotec) according to the manufacturer's instructions. The resulting preparations contained approximately 60% epithelial cell adhesion molecule-positive cells and less than 10% thymocytes (i.e., CD4/CD8 single-positive and CD4/CD8 double-positive cells) as determined by flow-cytometric analysis.

Real-time PCR. RNA was extracted from TECs with the High Pure RNA Isolation Kit (Roche Applied Science) and made into cDNA with the cDNA Cycle Kit (Invitrogen Corp.) according to the manufacturer's instructions. Real-time PCR for quantification of tissue-specific antigen genes was carried out as previously described (14). The primers and the probe for *PDIp* were as follows: primers, 5'-AGGCCAAAATAATTCAGCACATG-3' and 5'-TTTGTGAACCAGACACTAGCTCAAC-3'; probe, 5'-FAM-TCCACCAT-TACGAACAACACCTGCCC-3'.

CY-induced diabetes. CY (Sigma-Aldrich) dissolved in PBS was injected i.p. (0.2 mg/g body weight) into mice on day 0 and day 14. Mice were diagnosed as diabetic when blood glucose levels exceeded 250 mg/dl. Observation was terminated 28 days after the first CY injection.

Transfer of peripheral T cells into NOD scid mice. Thy1⁺ cells were isolated from the spleen, as previously described (38). In brief, the spleen cell suspensions were depleted of rbcs by osmotic lysis, and their Thy1⁺ cells were purified with CD90 (Thy1.2) MicroBeads (Miltenyi Biotec). The resulting preparations con-

tained approximately 95% Thy1$^+$ cells. The purified Thy1$^+$ cells were injected i.v. (4 × 10^6 cells per mouse), and development of diabetes was monitored for 20 weeks. Diagnosis of diabetes was performed as described above.

Measurement of serum Ig levels. The concentrations of Ig in the sera were measured by a sandwich ELISA using a clonotyping system with HRP (Southern Biotechnology Associates Inc.), as previously described (38).

Identification of autoantigen. Gastric epithelial cells were recovered by scratching of the surface of the glandular stomach from BALB/c mice with microscope slides. The cells were lysed in buffer containing 1% NP-40, 10 mM Tris-HCl (pH 7.4), 0.4 mM EDTA, 0.15 M NaCl, 10 μg/ml aprotinin, 10 μg/ml leupeptin, and 1 mM phenylmethylsulfonyl fluoride, and the mixture was then centrifuged for 10 minutes at 20,000 g. The supernatant was applied to DE52 resin (Whatman) that had been equilibrated with buffer containing 50 mM Tris-HCl (pH 8.0), hereafter referred to as buffer A. Proteins were eluted from the column stepwise with buffer A supplemented with 0.05–0.5 M NaCl. Fractions containing autoantigen were determined by Western blot analysis. One milliliter of the fraction containing autoantigen (i.e., the fraction eluted with 0.15 M NaCl) was concentrated and then applied to an Immobiline DryStrip (GE Healthcare) (pI 3–10) using Ettan IPGphor II (GE Healthcare). After isoelectric focusing electrophoresis, proteins were separated by SDS-PAGE on a 9% gel and stained with Coomassie brilliant blue. The stained spot corresponding to the autoantigen determined by Western blot analysis was excised from the gel. The protein was subjected to in-gel reduction, S-carboxyamidomethylation, and digestion with trypsin. The resulting

peptides were analyzed by LCQ ion-trap mass spectrometry (Thermo Electron Corp.) (39). N-glycosidase F treatment (Roche Molecular Biochemicals) was then carried out at 37°C for 24 hours.

Statistics. Statistics were analyzed with 2-tailed Student's *t* test; *P* values less than 0.05 were considered significant.

Address correspondence to: Mitsuru Matsumoto, Division of Molecular Immunology, Institute for Enzyme Research, University of Tokushima, 3-18-15 Kuramoto, Tokushima 770-8503, Japan. Phone: 81-88-633-7432; Fax: 81-88-633-7434; E-mail: mitsuru@ier.tokushima-u.ac.jp.

S. Niki and K. Oshikawa contributed equally to this work.

1. Eisenbarth, G.S. 1986. Type I diabetes mellitus. A chronic autoimmune disease. *N. Engl. J. Med.* 314:1360–1368.
2. Tisch, R., and McDevitt, H. 1996. Insulin-dependent diabetes mellitus. *Cell* 85:291–297.
3. Atkinson, M.A., and Leiter, E.H. 1999. The NOD mouse model of type I diabetes: as good as it gets? *Nat. Med.* 5:601–604.
4. Anderson, M.S., and Bluestone, J.A. 2005. The NOD mouse: a model of immune dysregulation. *Annu. Rev. Immunol.* 23:447–485.
5. Todd, J.A., and Wicker, L.S. 2001. Genetic protection from the inflammatory disease type I diabetes in humans and animal models. *Immunity* 15:387–395.
6. Kishimoto, H., and Sprent, J. 2001. A defect in central tolerance in NOD mice. *Nat. Immunol.* 2:1025–1031.
7. Zucchelli, S., et al. 2005. Defective central tolerance induction in NOD mice: genomics and genetics. *Immunity* 22:385–396.
8. Liston, A., et al. 2004. Generalized resistance to thymic deletion in the NOD mouse: a polygenic trait characterized by defective induction of Bim. *Immunity* 21:817–830.
9. von Boehmer, H., et al. 2003. Thymic selection revisited: how essential is it? *Immunol. Rev.* 191:62–78.
10. Björses, P., Aaltonen, J., Horelli-Kuitunen, N., Yaspo, M.L., and Peltonen, L. 1998. Gene defect behind APECED: a new clue to autoimmunity. *Hum. Mol. Genet.* 7:1547–1553.
11. Pirkänen, J., and Peterson, P. 2003. Autoimmune regulator: from loss of function to autoimmunity. *Genes Immun.* 4:12–21.
12. Ramsey, C., et al. 2002. Aire deficient mice develop multiple features of APECED phenotype and show altered immune response. *Hum. Mol. Genet.* 11:397–409.
13. Anderson, M.S., et al. 2002. Projection of an immunological self-shadow within the thymus by the Aire protein. *Science.* 298:1395–1401.
14. Kuroda, N., et al. 2005. Development of autoimmunity against transcriptionally unrepressed target antigen in the thymus of Aire-deficient mice. *J. Immunol.* 174:1862–1870.
15. Kyewski, B., and Derbinski, J. 2004. Self-represen-

tation in the thymus: an extended view. *Nat. Rev. Immunol.* 4:688–698.
16. Derbinski, J., et al. 2005. Promiscuous gene expression in thymic epithelial cells is regulated at multiple levels. *J. Exp. Med.* 202:33–45.
17. Liston, A., Lesage, S., Wilson, J., Peltonen, L., and Goodnow, C.C. 2003. Aire regulates negative selection of organ-specific T cells. *Nat. Immunol.* 4:350–354.
18. Anderson, M.S., et al. 2005. The cellular mechanism of Aire control of T cell tolerance. *Immunity.* 23:227–239.
19. Nakayama, M., et al. 2005. Prime role for an insulin epitope in the development of type I diabetes in NOD mice. *Nature.* 435:220–223.
20. DeSilva, M.G., et al. 1996. Characterization and chromosomal localization of a new protein disulfide isomerase, PDIp, highly expressed in human pancreas. *DNA Cell Biol.* 15:9–16.
21. DeSilva, M.G., Notkins, A.L., and Lan, M.S. 1997. Molecular characterization of a pancreas-specific protein disulfide isomerase, PDIp. *DNA Cell Biol.* 16:269–274.
22. Jiang, W., Anderson, M.S., Bronson, R., Mathis, D., and Benoist, C. 2005. Modifier loci condition autoimmunity provoked by Aire deficiency. *J. Exp. Med.* 202:805–815.
23. Kajiura, F., et al. 2004. NF-κB-inducing kinase establishes self-tolerance in a thymic stroma-dependent manner. *J. Immunol.* 172:2067–2075.
24. Harada, M., and Makino, S. 1984. Promotion of spontaneous diabetes in non-obese diabetes-prone mice by cyclophosphamide. *Diabetologia.* 27:604–606.
25. Yasunami, R., and Bach, J.F. 1988. Anti-suppressor effect of cyclophosphamide on the development of spontaneous diabetes in NOD mice. *Eur. J. Immunol.* 18:481–484.
26. Christianson, S.W., Shultz, L.D., and Leiter, E.H. 1993. Adoptive transfer of diabetes into immunodeficient NOD-scid/scid mice. Relative contributions of CD4$^+$ and CD8$^+$ T-cells from diabetic versus prediabetic NOD.NON-Thy-1a donors. *Diabetes.* 42:44–55.
27. Gallegos, A.M., and Bevan, M.J. 2004. Central tolerance to tissue-specific antigens mediated by direct

and indirect antigen presentation. *J. Exp. Med.* 200:1039–1049.
28. Jordan, M.S., et al. 2001. Thymic selection of CD4$^+$CD25$^+$ regulatory T cells induced by an agonist self-peptide. *Nat. Immunol.* 2:301–306.
29. Apostolou, I., Sarukhan, A., Klein, L., and von Boehmer, H. 2002. Origin of regulatory T cells with known specificity for antigen. *Nat. Immunol.* 3:756–763.
30. Sakaguchi, S. 2004. Naturally arising CD4$^+$ regulatory T cells for immunologic self-tolerance and negative control of immune responses. *Annu. Rev. Immunol.* 22:531–562.
31. Setoguchi, R., Hori, S., Takahashi, T., and Sakaguchi, S. 2005. Homeostatic maintenance of natural Foxp3$^+$ CD25$^+$ CD4$^+$ regulatory T cells by interleukin (IL)-2 and induction of autoimmune disease by IL-2 neutralization. *J. Exp. Med.* 201:723–735.
32. Shoda, L.K., et al. 2005. A comprehensive review of interventions in the NOD mouse and implications for translation. *Immunity.* 23:115–126.
33. Wang, J., et al. 2005. Establishment of NOD-Pdcd1$^{-/-}$ mice as an efficient animal model of type I diabetes. *Proc. Natl. Acad. Sci. U. S. A.* 102:11823–11828.
34. Liston, A., et al. 2004. Gene dosage-limiting role of Aire in thymic expression, clonal deletion, and organ-specific autoimmunity. *J. Exp. Med.* 200:1015–1026.
35. Vinuesa, C.G., et al. 2005. A RING-type ubiquitin ligase family member required to repress follicular helper T cells and autoimmunity. *Nature.* 435:452–458.
36. Heino, M., et al. 2000. RNA and protein expression of the murine autoimmune regulator gene (Aire) in normal, RelB-deficient and in NOD mouse. *Eur. J. Immunol.* 30:1884–1893.
37. van Vliet, E., Melis, M., and van Ewijk, W. 1984. Monoclonal antibodies to stromal cell types of the mouse thymus. *Eur. J. Immunol.* 14:524–529.
38. Yamada, T., et al. 2000. Abnormal immune function of hemopoietic cells from a lymphoplasia (aly) mice, a natural strain with mutant NF-κB-inducing kinase. *J. Immunol.* 165:804–812.
39. Matsumoto, M., et al. 2005. Large-scale analysis of the human ubiquitin-related proteome. *Proteomics* 5:4145–4151.